SOME ASPECTS OF MACHINING WITH SINGLE ABRASIVE GRAINS SIMULATING FINE GRINDING

By
J P SINHA

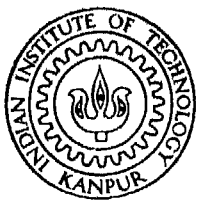

DEPARTMENT OF MECHANICAL ENGINEERING
INDIAN INSTITUTE OF TECHNOLOGY, KANPUR
NOVEMBER, 1976

SOME ASPECTS OF MACHINING WITH SINGLE ABRASIVE GRAINS SIMULATING FINE GRINDING

A Thesis Submitted
In Partial Fulfilment of the Requirements
for the Degree of
MASTER OF TECHNOLOGY

By
J P SINHA

to the
DEPARTMENT OF MECHANICAL ENGINEERING
INDIAN INSTITUTE OF TECHNOLOGY, KANPUR
NOVEMBER, 1976

ME-1976-M-SIN-SOM

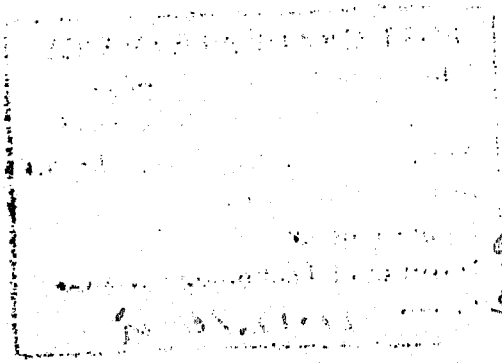

CERTIFICATE

This is to certify that the work entitled "SOME ASPECTS OF MACHINING WITH SINGLE ABRASIVE GRAINS SIMULATING FINE GRINDING" has been carried out under our supervision and has not been submitted elsewhere for the award of a degree

B. SAHAY
Assistant Professor
Dept of Mech. Engg
I I T. Kanpur

G K LAL
Assistant Professor
Dept of Mech Engg
I I T Kanpur

ACKNOWLEDGEMENT

I take this opportunity to express my deep sense of gratitude and sincere thanks for the invaluable assistance, that I have received, at the worthy hands of my honourable and learned guides Dr G K Lal and Dr B Sahay and for their continued interest in imparting me proper and useful guidance, encouragement and constant inspiration throughout the working on my thesis project, which would not have been, what it is, without their esteemed guidance

I am extremely thankful to Dr G S Kainth for devoting his valuable time, for very useful discussions and timely guidance at various stages

I acknowledge with grateful thanks for the invaluable cooperation and help which I have received from Messrs J. Singh, B P Vishwakarma, O P. Bajaj, D.K. Sarkar and S S Kushwaha

I shall be failing in my duty if I do not express my sincere thanks for the untiring zeal and efforts of Shri R M Jha and Shri B L Arora

I am also thankful to my colleagues, who have been most helpful, especially Shri B K Chaudhary and Shri D N P Sinha

In the end I wish to put on record my thanks to Mr. Uma Raman Pandey for his flawless typing

TABLE OF CONTENTS

LIST OF FIGURES AND TABLES

NOTATION

A	Maximum chip area of cut
A_g	Chip area of cut at depth g (in.)
A_c	Projected contact area
b	Maximum width of cut
$\bar{b}$	Mean chip width
b_g	Width of cut at depth g (in.)
C	Number of cutting grains per sq in.
c	Viscious damping coefficient
D	Wheel diameter
D_f	Damping factor
d	Maximum depth of cut
E	Young's Modulus of Elasticity
F_n	Normal cutting force
F_t	Tangential cutting Force
$F_o(t)$	Force acting on piezo-electric crystal
F(t)	Input grinding force
g	Depth from lowest point of cut
h	Height of drop
K	Spring stiffness of accelerometer
K_m	Static rigidity of dynamometer
N	Spindle speed of Aluminum disc
P_{max}	Maximum impact force
r	Ratio of width of cut to mean undeformed chip thickness
L	Sliding length

l	Length of cut
M	Material removal rate
m	Mass of the vibrating system of the accelerometer
S	Nominal grain size
T_k	Temperature at the surface of the workpiece
t	Maximum undeformed chip thickness
$\bar{t}$	Mean undeformed chip thickness
t_g	Undeformed chip thickness at depth g
u	Specific energy per unit volume of cut
V	Peripheral velocity of wheel
V_o	Volume worn out of the grinding wheel
v	Feed of workpiece
w	Frequency of the input force (circular)
w_n	undamped circular natural frequency of accelerometer
Z_T	Decay Rate
ρ	Grain tip radius
$\bar{\rho}$	Mean grain tip radius
τ	Shear stress
σ_n	Normal stress
$\Delta V'$	Rate of metal removal per unit time between two dressing cycle

μ	Poisson's Ratio
R_a	Maximum peak to valley height
x_o	Amplitude of forcing function
x_g	Displacement of the base from equilibrium position
x	Absolute displacement of mass of the accelerometer from static equilibrium position at any instant
x_R	Relative displacement of mass relative to the base
η	Frequency ratio
λ	Metal removal parameter
α	Distance of approach
α_1	Distance of approach at the instant of maximum compression
V'	Gain factor
R_a^{β}	Surface roughness with sparkout
T_{max}	Maximum temperature during grinding

SYNOPSIS

In fine grinding, specific energy, wheel wear and temperature rise appear to be directly related to the cutting forces. In grinding, however, the effect of individual grains cannot be accounted for since several grains are simultaneously in contact. In order to analyse the mechanics of the grinding process, it is, therefore, imperative that the mechanics of chip formation with single abrasive grains be evaluated. One of the most important parameters is obviously the force that acts at the grain-chip interface. There are many difficulties in experimentally measuring these forces since their magnitude is usually very small (1/2 kg or so) and the duration in most cases is less than 100 μ sec.

In the present work it has been shown that a piezoelectric accelerometer can be successfully used for measuring these forces. It has also been shown that the displacement of the accelerometer is proportional to the input force and that the dynamometer can be calibrated by dropping a ball from known heights.

Overcut flymilling experiments indicate that the tangential force on a grain varies approximately linearly with the chip cross-section area. The specific energy and shear force increase with decrease in chip size in a similar manner as reported earlier for

fine grinding Normal or contact stress on the other hand remains more of less constant with chip thickness except in the range of very fine chip thickness where it increases with decreasing chip size

In this regards, the overcut flymilling technique where a single abrasive grain is mounted on the periphery of an aluminum[1] disc and used as a grinding wheel appears to be very useful This closely approximates fine grinding conditions

CHAPTER I

I 1 0 INTRODUCTION

In comparison with most other machining processes, grinding has received far less attention by research workers This is no doubt due to its inherent complexity However, the trends towards ever increasing precision in manufacturing, use of various types of materials, some of them even difficult to machine, and the smaller stock allowances on primary shape are now stimulating further interest in this machining operation

This process is unique, since it depends on the action of individual grains of very hard abrasive materials such as Alumina, Silicon Carbide, or even diamond, held together by a bonding agent It is basically a chip forming process, but very brittle work materials may disintegrate into dust particles The chips are produced by the slightly protruding portions of numerous irregularly shaped and randomly spaced abrasive particles. Thus the dimensions of the chips formed under a particular set of grinding conditions vary widely In typical precision grinding operations, the chips are thin and narrow, but under stock removal conditions such as billet grinding, the chips can be as thick and wide as those obtained in

multi-tool cutting operations like milling If sparking occurs, as during grinding of mild steel, the distribution of chip sizes available for examination is affected by preferential ignition or melting of the thinner chips

The dimensions of the deformed grinding chips for a particular set of grinding conditions depend on several factors One is the number of cutting elements per unit area of the wheel surface that are present in a layer whose thickness is related to that of the thickest chips produced. This includes not only the relatively few particles that would contact a smooth, flat surface when the wheel is rolled over it, but also those particles that do not quite extend this far and yet happen to be favourably situated to produce chips The deeper a grit is below the outer most surface of the wheel, the higher is the probability that an abrasive grain will not contact the work piece This is primarily because a more protruding grain immediately ahead of it has already removed the material

The elastic deflection of the bond posts holding the grains in place, caused by the forces acting on the wheel is another factor that affects the location of some of the grains and hence their availability for cutting[1,2] Also, more than one cutting elements may be present on an individual grain, so that the number of

chips produced by that grain will depend on the deepest cut it happens to take Finally, the chip dimensions will depend on the extent to which it is deformed as it is being produced

Not all grains that come in contact with the work surface will produce chips When there is insufficient interference between a grain and the work, a ploughing action may result in which the metal is pushed aside and some of it comes off as irregular and highly distorted particles without chip being formed[3] The shape of the cutting element is one factor in determining whether cutting or ploughing takes place Some abrasive grains will not be in position to more than deform the surface elastically, in which case there will only be a rubbing action without any metal removal

I 2 0 THE INFLUENCE OF UNDEFORMED CHIP-THICKNESS IN GRINDING

In grinding, a number of researchers have investigated the significance of undeformed chip thickness which may be derived directly from the grinding conditions, on the grinding output[4,5,6] The important grinding outputs are, **G**rinding forces, **S**pecific energy, **R**elative wheel **H**ardness, **W**heel wear, **S**urface roughness (finish), and **G**rinding temperatures.

I.2 1 GRINDING FORCES AND ENERGY

Specific cutting energy (u) is a useful concept in turning and other metal cutting operations since it has essentially a constant value for a wide variety of cutting conditions If specific energy is known for a given tool-workpiece combination, then the cutting forces corresponding to a wide variety of cutting conditions may be readily calculated or vice-versa Specific cutting energy is an equally important quantity in grinding While u is essentially independent of the undeformed chip thickness in single point cutting operations, it is functionally related to the mean undeformed chip size, $\bar{t}$, in grinding In the practical grinding range, it has been shown[7] that

$$u = k'(\bar{t})^{-n} \qquad (1\ 1)$$

where k' is constant for a given wheel-workpiece combination, independent of chip thickness. The value of n has been shown to be approximately equal to 0 9 for fine grinding and 0 5 for coarse abrasive machining[7]

The (u) vs ($\bar{t}$) plot is valuable, since it enables horsepower (P) and force requirements to be estimated for any combination of operating variables, or vice-versa.

The forces acting on a grinding wheel have been discussed by Marshall and Shaw[8]. The following equations have been suggested for estimating these forces :

$$F_t = u\ b\ d\ \frac{v}{V} \qquad (1.2)$$

$$F_n = k_1\ F_t \qquad (1.3)$$

Here F_t and F_n are the tangential and normal components of grinding force, v and V are the table and wheel speeds, b is the width of cut, d is the wheel depth of cut and k_1 is a constant.

For a particular combination of wheel-workpiece and kinematical conditions, it can be shown that these forces are function of undeformed chip thickness. The equation for maximum undeformed chip thickness (t) for surface grinding (Fig.1) can be written as[8]

$$t = \sqrt{\frac{4\ v}{VCr}}\sqrt{\frac{d}{D}} \qquad (1.4)$$

where r is the ratio of width of cut and mean undeformed chip thickness ($\bar{t}$), C is the number of cutting grits per unit area of the wheel surface and D is the wheel diameter. The specific energy (u) can be evaluated from

$$u = \frac{F_t\ V}{vbd} \qquad (1.5)$$

Using equations (1.4) and (1.5), equations (1.2) and (1.3) reduce to

$$F_t = k_3 (\bar{t})^{-n+2} \qquad (1.6)$$

$$F_n = k_4 (\bar{t})^{-n+2} \qquad (1.7)$$

where k_3 and k_4 are constants.

I.2.2 RELATIVE WHEEL HARDNESS

The mean force acting on a single abrasive grain in grinding wheel is of importance in relation to wheel hardness and fracture or attritious wear of abrasive grains. It has been shown by Reichenbach et al[4] that the mean tangential force F_g on a grain may be obtained by the following equation

$$F_g = \frac{u}{4} (\bar{t})^2 r \qquad (1.8)$$

or

$$F_g = k_5 (\bar{t})^{-n+1} \qquad (1.9)$$

Equation (1.9) has been derived with the help of equation (1.1). Here k_5 is a constant.

This indicates that the mean tangential force, F_g, or the maximum force approximated equal to 2 F_g is a function of undeformed chip thickness. Since it has been shown that $n < 1$, the exponent of $\bar{t}$ in the equation (1.9) will always have a positive value. By increasing the value F_g i.e. by increasing the undeformed chip

thickness a given wheel may be made to behave as "Soft". Therefore, the principal ways of decreasing the effective hardness of a grinding wheel are

1) To increase the work speed (v)
2) To decrease the wheel speed (V)
3) To decrease the number of cutting points per unit area (C) on the wheel face by dressing or by changing the grain size or grain spacing
4) To increase the wheel depth of cut (d)

I.2.3 SURFACE ROUGHNESS

A major source of roughness of a surface ground on a stable machine will be the scallops left behind due to the finite spacing of successive grains. If all active grains extend the same distance from the wheel surface then plan view will consist of an array of very slender diamond shaped scratches (Figure 2). The point of all diamonds will lie in the same plane in this idealized model It has been shown by Snoeys[6] that average roughness for a particular wheel-work combination and constant kinematical conditions, is a function of mean or maximum undeformed chip thickness which in mathematical form can be stated as

$$R_a = R_1 (\bar{t})^{\nu} \qquad (1\ 10)$$

where R_a is the maximum peak-to-valley height, R_1 and γ are constants for a particular grinding ratio and stock removal conditions

With spark out this is of the form

$$R_a^{\beta} = R_1^1 \left(\frac{1}{t} \right)^{\gamma\beta} \qquad (1\ 11)$$

where R_1^1 is a constant

I 2 4 WHEEL WEAR

In grinding, wear is an integral part of the process, and a wear rate that is too slow can be more undesirable in its consequences than a rapid one Generally three types of abrasive wear are identified They are (i) attritious wear, (ii) fracture wear, and (iii) bond failure

Attritious wear is wear of small magnitude in which flat surface is produced by mechanical or chemical action, on the portion of the abrasive grain that comes in contact with the workpiece Grain fracture is a sharpening mechanism in which a new cutting edge is formed by fracture of an individual abrasive grain During bond failure, the entire remaining portion of an abrasive grain, or aggregates of several grains, are removed from the grinding wheel matrix by mechanical failure of the supporting bond posts(1)

Many parameters have been used to study abrasive wear One parameter used is ratio of volume worn out per unit sliding length to the total normal load Mathematically this has been represented as[9]

$$\frac{V_o}{LF_n} = \frac{V_o}{LK_1F_t} = \frac{1}{(\text{Constant})\ u}$$

or $$\frac{V_o}{LF_n} = k_6 \left(\bar{t}\right)^n \qquad (1\ 12)$$

where V_o and L are the volume worn out of the grinding wheel and sliding length, respectively

Thus it indicates that this wear parameter is also a strong function of undeformed chip thickness Equation (1 12) also implies that this parameter will have different values for a particular wheel-work combination, depending upon the types of grinding (rough or fine grinding)

Another parameter introduced to illustrate abrasive wheel wear mechanism is due to Hahn[10,11,12,13] which he called as "Metal Removal Parameter" (λ) It is defined as the ratio of the rate at which material is removed in grinding (M) to the normal force (F_n) on the grinding wheel. Thus λ can be expressed as,

$$\lambda = \frac{M}{F_n} \qquad (1\ 13)$$

In terms of specific energy this can be written as

$$\lambda = \frac{k_7 V}{u} \qquad (1\ 14)$$

where k_7 is constant

Thus for a particular work-wheel combination and kinematical conditions,

$$\lambda = k_8 (\bar{t})^n \qquad (1\ 15)$$

where k_8 is constant λ is therefore, directly proportional to the wear parameter This equation also, like the previous one, is a function of mean undeformed chip thickness

Another parameter specifying wheel wear has been introduced by co-operative research group of the C I R P Grinding Committee[6] It is the rate of metal removal per unit time ($\Delta V'$) between two dressing cycles It has been shown that this parameter is also a function of undeformed chip thickness and the relationship is of the form

$$\Delta V' = V_1 (\bar{t})^{\delta} \qquad (1\ 16)$$

where V_1 and the exponent δ are constants for a particular wheel-workpiece combination and kinematical conditions

I 2 5 GRINDING TEMPERATURES

Aside from the surface roughness aspects, the surface integrity of ground surface is equally important It has been shown[14] that roughly 85% of the total grinding energy is dissipated as heat flowing into the workpiece It is the main cause of structural damage and occurence of tensile residual stresses

In order to determine the dominant parameter in this respect, the grinding process has been analysed using a moving band heat source as described by Jaeger[15] This model has been shown[6] to be reasonably accurate for estimating the workpiece temperatures during surface and cylindrical grinding This analysis gives the maximum temperature of the workpiece (T_{max}) as,

$$T_{max} = T_k \, e^{-Z/Z_T} \qquad (1\ 17)$$

where T_k is the temperature at the surface given by the expression

$$T_k = T_o \, (\bar{t})^{\theta} \quad \alpha^{0.47}/K \qquad (1\ 18)$$

Z_T is a measure for its decay rate below the ground surface and is given by the expression,

$$Z_T = Z_o \, (\bar{t})^{0\ 37} \quad \alpha^{0\ 63} \qquad (1\ 19)$$

where T_o and Z_o are constants, Z is the depth under the

surface of the workpiece, α and k are the thermal diffusitivity and heat conductivity factor of the materials, respectively

This expression for the maximum temperatur indicates that it is also a function of undeformed chip thickness

It can thus be concluded that undeformed chip thickness plays a vital role in grinding The magnitude of mean undeformed chip thickness depends on the kinematic conditions such as work speed (v), wheel speed (V), wheel depth of cut (d), wheel diameter (D), surface topography represented by number of cutting edges per unit area (C) and the ratio of width of individual scratches to the mean undeformed chip thickness (r) Some of the factors influencing $\bar{t}$ such as v, V, d, D may be controlled easily but number of cutting edges per unit area (C), and the ratio 1 cannot be predicted accurately In the expression for determination of undeformed chip thickness ($\bar{t}$), equation (1 4) , some simplifying assumptions have been made, such as constant number of cutting edges per unit wheel surface area, constant distance between two succeeding cutting tips along the periphery of the wheel, and constant distance of cutting edges from the axis of the grinding wheel These simplifying assumptions reduce the grindirg process to a multi-toothed milling

process with large number of cutting points and small depth of cut But it is unfortunate that the principle of milling process does not apply to the grinding process Due to random cutting geometry, the orientation of cutting grains on the surface may be totally unsuitable for chip formation Some grain will lie too far below the general level of the neighbouring grain to contact the metal, while unfavourable geometry may cause others to break off on first contact with workpiece, or only slide rather than form chip It was also shown by Nakayama and Shaw[16] that the number of active cutting edges decrease very rapidly at small undeformed chip thickness.

I 3.0 PRESENT WORK

Although the undeformed chip thickness is the most important parameter in evaluating the grinding performance, specific energy, wheel wear and temperature are actually influenced by the forces acting at the wheel-work interface This force is the cumulative effect of forces acting on individual grain in the interface region While specific energy and temperature are directly related to the grinding forces in the form of mechanical energy, the wear mechanism of a wheel depends on the force on an individual grain Depending upon the magnitude of this force, the wear may be attritious or fracture in nature Thus the knowledge of the magnitude and variation of this force with grinding conditions is of paramount interest

from the point of view of performance of grinding wheels

Many attempts have been made[8,17] to measure these forces during grinding where several grains act at the wheel-work interface In order to understand the mechanics involved in the process, it is necessary to study the grinding force on an individual grain Very little appears to be known about this aspect primarily because of difficulities involved in accurate measurements of forces of very small magnitude ($\simeq$ 1/2 kg) acting for a very short time (100μ sec)

In this study an attempt has been made to measure the forces acting on an individual grain with the help of an accelerometer. The over cut fly-milling technique has been used where the grinding wheel is replaced by an aluminum disc with a grain attached to its periphery The grain removes a chip like in surface grinding Special technique had to be developed for mounting grain (approximately 1 mm in diameter) on the aluminum disc The work was then extended to study the effect of various parameters on forces acting on an individual grain

CHAPTER II

II 1

The action of a single abrasive grit embedded in the surface of a grinding wheel may be approximated by one of three separate flymilling operations where the milling tooth is replaced by a single grit mounted on the periphery of a circular disk The three flymilling operations are (i) Plane, (ii) Overcut, and (iii) Face flymilling as shown in Fig 3

In plane flymilling the grit experiences a large dynamic shock load during each revolution of the disc During face flymilling the length of cut is much greater, and closely resembles the situation in the abrasive cut-off operations In over-cut flymilling, the length of engagement approximates more closely to that which exists during horizontal spindle surface grinding

Since overcut flymilling closely resembles fine surface grinding operations, this operation was selected to study the cutting action of single grit

II 2 EXPERIMENTAL SET UP

The cutting was performed on a H M T horizontal milling machine having specification shown in Table 1 An aluminum disc of outer diameter and thickness of 250 mm and 24 mm respectively was mounted on the spindle

of the milling machine The outer periphery of the aluminum disc bore two diametrically opposite tapped holes for attaching a single grit mounted in the cavity of the socket head screw The workpiece was held in a vice and traversed horizontally so that the cutting action was similar to that in surface grinding or in overcut flymilling The general arrangement is shown in Figure 8

Before cutting, the surfaces of the workpiece was ground to a fine finish and taper of 1 mm in 127mm and 1 27 mm. in 254 mm were provided at the top and side faces respectively covering nearly half of the entire surface area of the faces A sharp clearly visible line separated the taper and the flat faces as shown in Figure 3 (C)

II 2 1 MOUNTING TECHNIQUE OF THE GRAINS

Number 14 size grain of black Al_2O_3 were used The grain was mounted in the head of a small Allen head screw by use of two cements After cleaning the Allen head with Acetone, the cavity was coated with a thin layer of expoxy cement (Araldite brand) and then filled with Sauereisen (Electric Register No 63) ceramic cement The grain was then lightly pushed into the cement and air dried for 24 hours

II 3 DYNAMICS AND DESIGN OF DYNAMOMETER

For the experimental estimation of the grinding forces due to cutting action of abrasive grains, it is essential to measure the impulsive force of low magnitude (approximately 1/2 kg) which acts on the individual cutting edges for a very short time (approximately 50 sec) The dynamometer should, therefore, be capable of measuring such impulsive forces with some acceptable degree of accuracy The dynamometer thus designed should incorporate the following basic features

Influence of the dynamometer on the system under observation should be minimum i e the instantaneous history of the set grinding depth of cut should not be changed, thus affecting the grinding parameters From this view point it is ideal that the dynamometer be so rigid as not to be deflected appreciably by the working force and at the same time be able to detect that working force precisely Shiozaki and Miyashita[18] have shown that for minimum influence of the dynamometer on the system under observation, the static rigidity (km) should satisfy the following condition i e

$$km < \frac{1}{2D_f} \times \text{cutting force per unit depth of cut} \qquad (2\ 1)$$

Assuming, the cutting force (normal component) per micron depth of cut to be of the order of 100 g (16), and

damping factor of 0 7,(16)

$$km \gg 0.07 \text{ kg}/\mu\text{M} \qquad (2\ 2)$$

In order to make the dynamometer have static rigidity enough to meet equation (2 2), it is necessary for the stiffness of the support of the workpiece to be high Assuming the support of the workpiece to be a fixed beam as shown in Figure 8, the static rigidity of the support (km) equals to 274 kg/μM, which satisfies the equation (2 2)

Influence of the dynamometer on the cutting force applied to the workpiece is another features of paramount importance The response of the dynamometer should be least affected and should correspond accurately and faithfully to the input cutting force

The schematic diagram of the dynamometer used during the present investigation is shown in Figure 8 in which a Piezo-Electric-Accelerometer (Type 4334, S No 301251, manufactured by Bruel & Kjaer, Denmark) having calibrated undamped natural frequency of 48 KHZ has been used. For a practical treatment, the dynamometer can be assumed as equivalent to a single degree of freedom system inside a case which has been fastened rigidly to the vibrating system through which the cutting forces are transmitted as shown in Figure 5

Applying Newton's second law of motion to the equivalent system for the dynamometer, we have

$$mx = - c (x - x_g) - k (x - y_g) \qquad (2\ 3)$$

where m, c, k, x and x_g are the mass of the vibrating system, viscious damping coefficient, equivalent stiffness of the spring, absolute displacement of the mass from the static equilibrium position at any instant and displacement of the base from an equilibrium position at the same instant, respectively For the purpose of analysis the cutting force applied to the workpiece can be assumed to be harmonic, and in terms of displacement it can be represented by the equation,

$$x_g = x_o \sin wt \qquad (2\ 4)$$

where x_o is the amplitude of the harmonic force, w is the circular frequency of vibration of the cutting force Equation (2 3) can now be converted into a dimensionless form by substituting

$$w_n^2 = k/m \qquad (2\ 5)$$

$$\tau = w_n t \qquad (2\ 6)$$

$$\frac{dx}{dt} = x = w_n \frac{dx}{d\tau} \qquad (2\ 7)$$

$$\frac{d^2x}{dt} = \ddot{x} = w_n^2 \frac{d^2x}{d\tau^2}$$

$$\eta = \frac{w}{w_n} \qquad (2\ 8)$$

and $$D_f = \frac{c}{2(km)^{1/2}} < 1 \qquad (2\ 9)$$

where τ is the dimensionless time, η is the ratio of the cutting force frequency to the undamped natural frequency of the accelerometer and D_f is the damping ratio The equation (2.3) now takes the form of

$$x'' + 2D_f x' + x = x_o \sin \eta\tau + 2D \eta x_o \cos \eta\tau \qquad (2\ 10)$$

The co-ordinate x here yields the measured displacement of the mass m compared with an inertial system It is difficult to measure and the output voltage is not proportional to this displacement and thus is of no interest. For our purpose the relative motion x_R of the mass, m, compared with that of the base will be of interest The output voltage of the accelerometer obviously corresponds to this relative displacement

Thus $$x_R = x - x_g \qquad (2.11)$$

Substituting equation (2 11) in equation (2 10), we get

$$x_R'' + 2D_f x_R'' + x_R = x_o \eta^2 \sin \eta\tau \qquad (2\ 12)$$

The general solution of this equation is obtained as the summation of the solution obtained for the free vibration (complementary function) and a particular integral It can be shown that the general solution of the equation (2 12) will be of the form

$$x_R = x_o \; V' \sin(\eta\tau - \psi) + A\, e^{-D\eta\tau} \sin\left[(1-D_f^2)^{1/2}\tau + \phi\right] \qquad (2\ 13)$$

where V' is the magnification or gain factor, given by the equation

$$V' = \frac{\eta^2}{\left[(1-\eta^2)^2 + 4 D_f^2 \eta^2\right]^{1/2}}$$

and ψ is the phase angle, given by the expression

$$\tan\psi = \frac{2 D_f \eta}{1 - \eta^2} \qquad (2\ 14)$$

A and ϕ are constants which can be determined from the initial conditions Considering initial conditions of $x_R(o) = o$ and $x_R'(o) = o$ the constants A and ϕ are (2 15)

$$A = x_o V' \sqrt{\sin^2\psi + (\tan\theta \sin\psi - \eta \sec\theta \cos\psi)^2}$$

$$\tan\phi = \frac{1}{\tan\theta - \eta \cos\theta \quad \cot\psi} \qquad (2\ 16)$$

where $\tan\theta = \dfrac{D_f}{(1-D_f^2)^{1/2}}$ (2 17)

These equationsmay be further simplified by considering the actual damping ratio D_f utilised by the accelerometers, and the frequency ratio η . Most accelerometers utilize damping ratio near $D_f = 0\ 7$[19] which not only extends the useful ffequency range but prevents phase distortion and the factor

$\dfrac{1}{\left[(1-\eta^2)^2 + 4 D^2 \eta^2\right]^{1/2}}$ remains equal to 1 for frequency ratio range of $\eta = o$ to $\eta = 0\ 2$[19]

In case of overcut flymilling the length of cut (l) is given by the expression

$$l \simeq \sqrt{D\,d} \qquad (2\ 18)$$

where D is the wheel diameter and d is the wheel depth of cut The cutting time (T) for a single cut is given by

$$T = \frac{l}{V}$$

where V is the peripheral velocity of the cutting edges considering the wheel diameter of 264 mm, wheel depth of cut of 0 025 mm, and other cutting conditions shown in Table 4, the frequency of the cutting force comes to 0 162 KHZ The frequency ratio η then is equal to

$$\eta = 0\ 00348$$

or $$\eta \ll 1$$

Substituting in equations (2 14), (2 15), (2 16) and (2 17) we get

$$\psi = o$$

$$\theta = \pi/2$$

$$\phi = o$$

$$A = \frac{-\ {}_{o}V'\gamma_1}{(1-D^2)^{1/2}}$$

Substituting this equation (2 13) is transformed to

$$x_R = \frac{x_o\ w^2}{w_n^2}\left[\sin wt - \frac{w}{w_n(1-D_f^2)^{1/2}}\ e^{-Dw_n t}\sin (1-D_f^2)^{1/2} w_n t\right]$$

(2 20)

This equation shows that for subcritical running $\eta \ll 1$, the vibrometer functions as an accelerometer It can also be seen that the magnitude of the second term in the square brackets is small enough in comparison to the first term Since the instrument is tuned to a high frequency, the mass follows the motion of the base of the instrument quasi-statically and the accelerating forces of the mass are measured by the spring system Thus the system can be used as a dynamometer where the applied force is proportional to the deflection of the spring The output voltage is proportional to the force applied to the piezo-electric element[20] and in turn proportionate to the output response x_R Thus,

$$V(t) \propto F_o(t) \qquad (2\ 21)$$

and $$F_o(t) = k\, x_R \qquad (2\ 22)$$

where $F_o(t)$ is the force acting on the piezo-electric crystal and $V(t)$ is the corresponding output voltage Substituting x_R from the equation (2 20), we have

$$F_o(t) = m\, x_o\, w^2 \left| \sin wt - \frac{w\, e^{-D_f w_n t}}{w_n (1-D_f^2)^{1/2}} \right.$$

$$\left. \sin (1-D_f^2)^{1/2}\, w_n t \right| \qquad (2\ 23)$$

This equation shows that the force response $F_o(t)$ of the dynamometer may comprise the erratic damped ripple

of frequency $(1-D_{\zeta}^{2})^{1/2}\ w_n/2\pi$ as shown in Fig 6 These can, however, be reduced to negligible values by employing accelerometer of high natural frequency but at the cost of sensitivity Figure 7 shows the CRO traces for the normal and the tangential force components of the grinding force which very well corresponds to the theoretical output response given by the equation (2 23) and also corresponds to the input force $F(t) = F_o$ Sin wt

It is clear from the foregoing analysis that this arrangement with accelerometer can be utilized for measuring impulsive forces.

II 3 1 CALIBRATION OF DYNAMOMETER

Figure 8 shows the arrangements for mounting the workpiece on the dynamometer and the general view of the arrangements for measuring the cutting forces F_n and F_t. The principal axis of the accelerometers was adjusted carefully so that it was always along the line of action of the applied cutting force In this situation, the cross-sensitivity remains less than 2%

The method adopted to calibrate the dynamometer consists of impinging a stainless steel ball with known velocity against the workpiece and recording the signals from the dynamometer on a storage oscilloscope, (Type 564B, TEKTRONIX) Figure 9 shows the block diagrams for the measuring arrangements of the output response Table 2

shows the specifications of the elements of the measuring arrangements To impinge the ball with known velocity against the workpiece, the ball was dropped from a known height with no initial velocity Figure 10 shows the ball dropping device which gives good results The ball can be placed in position accurately by putting slip gauges of known thickness between it and the workpiece When the jaws of the device are opened, the ball falls freely from the tapered jaws

The impact force of a ball on the dynamometer is amenable to theoretical calculations Figure 11 shows the impact of two spheres in motion along the line joining the centres of the spheres As soon as the spheres, in their motion toward one another, come in contact at a point o, the compressive force P begins to act and changes the velocities of the spheres If v_1 and v_2 are the values of these velocities, their rate of change during impact are given by Newton's second Law of motion as

$$m_1 \frac{dv_1}{dt} = - P \qquad (2\ 24)$$

and

$$m_2 \frac{dv_2}{dt} = - P \qquad (2\ 25)$$

where m_1 and m_2 denote the masses of the spheres Let α be the distance the two sphere approach to one another due to local compression at o, then the velocity of approach is

$$\frac{d\alpha}{dt} = \dot{\alpha} = v_1 + v_2 \qquad (2.26)$$

From equations (2 24) and (2 25) we have

$$\ddot{\alpha} = \frac{d^2\alpha}{dt^2} = - P \frac{m_1 + m_2}{m_1 \; m_2} \qquad (2\ 27)$$

It is assumed that the duration of impact is very long in comparison with the period of lowest mode of vibration of the spheres Vibrations can, therefore, be neglected, and it can be assumed that the relation between force P and the distance of approach α which has been established for statical conditions[21], holds during impact and is given by

$$P = n' \alpha^{3/2} \qquad (2.28)$$

$$n' = \sqrt{\frac{16}{9\ \pi^2} \frac{R_1 R_2}{(k_1 + k_2)(R_1 + R_2)}} \qquad (2\ 29)$$

$$k_1 = \frac{1 - \mu_1^2}{\pi E_1} \qquad (2\ 30)$$

and $$k_2 = \frac{1 - \mu_2^2}{\pi E_2} \qquad (2\ 31)$$

Here R_1 and R_2 are the radii, μ_1 and μ_2 are the Poisson's ratio and E_1 and E_2 are the Young's Modulus of elasticity for the spheres Substituting equation (2 28) in equation (2 27), we get

$$\ddot{\alpha} = - n' n_1 \alpha^{3/2} \qquad (2\ 32)$$

where $$n_1 = \frac{m_1 + m_2}{m_1 \; m_2} \qquad (2\ 33)$$

Equation (2.32) is a differential equation and can be solved for the value of approach α_1 at the instant of maximum

compression The solution gives,

$$\alpha_1 = \left(\frac{5}{4}\,\frac{v'^2}{n' n_1}\right)^{2/5} \qquad (2\ 34)$$

where v' is the velocity of approach at the beginning of impact Now maximum compressive force can be estimated from equation (2 28) as

$$P_{max} = n' \alpha_1^{3/2} \qquad (2\ 35)$$

Solving equation (2.32) for the duration of impact (T), we get

$$T = 2.94\,\frac{\alpha_1}{v} \qquad (2\ 36)$$

Table 3 gives the mechanical and physical properties of the cold-rolled mild steel workpiece and the stainless steel ball used for experiment

Using this data, the expression for maximum impact force (P_{max}) reduces to

$$P_{max}\ (lb) = 1\ 313 \times h^{3/5} \qquad (2\ 37)$$

where h is the drop height in mm.

The calibration consists of correlating the maximum impact force at a particular drop height to the maximum output voltage recorded on the storage oscilloscope The calibration curve is given in Fig 12 It indicates that the maximum output voltage from the dynamometer is directly proportional to the maximum impact force The calibration constant comes to 152 2 mV/lb

II 4 PRELIMINARY EXPERIMENTS

After completing the necessary design as discussed previously, the required components were fabricated and assembled as shown in Figure 8, and was tested for proper working After satisfactory performance was achieved some preliminary tests were performed Figure 7 shows typical traces for normal and tangential force components

The actual depth of cut (d) during these and all subsequent tests was evaluated from the length of scratch produced on the tapered portion of the workpiece as shown in Fig. 3(C) The length of scratch in all cases was measured on an optical projector (140Y) with a micrometer base The least count available was 0 001 mm The maximum width of scratch (b) was also measured on the same projector

CHAPTER III

RESULTS AND DISCUSSION

A characteristic feature of abrasive grains used in the grinding wheels is their uncertain shape and size These are not only randomly distributed but also change continuously as grinding proceeds These grains belonging to the same nominal size may give entirely different data under otherwise identical cutting conditions

Results show a wide range of scattering in the tangential (F_t) and normal Force (F_n) with different grains scratching at the same depth , d (Fig. 13) All these grains were of Mess size 14 (nominal grain diameter 1 0 mm. These fluctuations in the force data are apparently due to the wide range of fluctuation in the maximum width of cut, b (Fig 14) Thus no meaningful result will be obtained from a plot of tangential force (F_t) versus depth of cut (d) unless the effect of variation in grain size is somehow eliminated During actual grinding tangential force has been found to increase with increasing depth of cut[17,22,23] In a grinding wheel several grains cut simultaneously thus the effect of variation in the size and shape of individual grains is not important

It has been shown[24] that grooves cut by single grains in overcut flymilling are closely approximated by

circular arcs A typical Talysurf trace of such a grooves is shown in Fig 15 thin grains on an average may be assumed to be spherical in shape and the radius at the tip of the grain ρ may be calculated from

$$\rho = \frac{d}{2} + \frac{b^2}{8d} \qquad (3\ 1)$$

Fig 16 shows the result obtained in sieve analysis of a sample of size 11 grains It indicates significant variation in grain diameter (g) and hence, ρ

Keeping these in view the maximum tangential force F_t was plotted against the maximum cross-sectional area of chip (Fig 17) This chip cross-sectional area, A, has been taken to be ($2\sqrt{2}\ \frac{v_d\sqrt{\rho}}{N\sqrt{D}}$) For this plot a close class interval of the cross-sectional area (A) is chosen Best straight line using least square method gave the relationship as

$$F_t = F_{t_o}\ A^{0\ 93} \qquad (3\ 2)$$

where F_{to} is a constan

Thus the tangential force is a function of the chip area of cut and this relationship could be approximated as

$$F_t \propto A \qquad (3\ 3)$$

This agrees with the assumption first proposed by Alden[25] to explain the behaviour of grinding wheels Many subsequent

investigators have used this assumption without verifying it experimentally. Equation (3.3) also implies that F_t is not only a function of depth of cut (d) but also a function of absolute grain size.

Thus to eliminate the effect of variation in grain size from the face data it is reasonable to assume that all cuts were made with a grit of a constant tip radius ($\bar{\rho}$), adjusted to having a modified depth of cut (d_m), such that the maximum area of cut remains the same. The grain tip radius ρ was obtained using the equation (3.1), which approximate the shape of the grains to be spherical. The constant tip radius was chosen to be the mean tip radius (87.8 x 10^{-4} inch) obtained. This mean tip radius comes to be of the same order as that given by

$$\rho = \frac{0.041}{s^{0.53}} \quad (28) \qquad (3.4)$$

where S is the nominal grain size. For 14 size grain equation 3.4 gives a value of 101 x 10^{-4} inches. Modified depth of cut d_m thus follows from the expression

$$d\sqrt{F} = d_m\sqrt{\bar{\rho}} \qquad (3.5)$$

and $\bar{\rho} = 101 \times 10^{-4}$ inch

$$d_m = \left(\frac{\rho}{\bar{\rho}}\right)^{1/2} d \qquad (3.6)$$

$$t_m = \frac{\rho^{1/4}\, t}{(101 \times 10^{-4})^{1/4}} \qquad (3\ 6a)$$

where t_m is the corrected undeformed chip thickness Using equation (3 6a) the corrected wheel depth of cut can be obtained Again a close class interval has been chosen for obtaining the variation of F_t with depth of cut (Fig 18). Least square curve fitting gave the relationship to be of the form

$$F_t = F_t' + F_t''\ d_m \qquad (3\ 7)$$

where F_t' and F_t'' are constants Substituting for d_m from equation (3 6) we get,

$$F_t = F_t' + F_{t_o}'' \frac{\rho^{1/2}}{\rho^{1/2}}\, t^2 \qquad (3.8)$$

since d $\simeq$ constant t^2 (3 9)

Referring to equation (1 6), it shows that tangential force is only a function of undeformed chickness But the experimental results show that tangential force (F_t) is not only a function of the undeformed chip thickness, but also of the grain tip radius The apparent discrepency between the results may be attributed to the variation of grain tip radius As the cut proceeds, wear flat develops thus increasing the grain tip radius It is assumed that fracture wear does not take place Equation (3.8)

further shows that for a constant undeformed chip thickness and thus for a constant wheel depth of cut, the maximum tangential force increases, which corresponds to the physical situations

Assuming the shear stress to be uniform over the entire cross-section of the undeformed chip, the shear stress (τ) can be evaluated from

$$\tau = \frac{F_t}{A} \qquad (3\ 10)$$

Variation of τ with corrected undeformed chipthickness (t_m) is shown in Fig 19 This yields the relationship

$$\tau = \tau_o\, t_m^{-0\ 826} \qquad (3\ 10a)$$

where τ_o is a constant The derivation of expression for undeformed chip thickness is given in Appendix-A and the corrected chip thickness t_m has been evaluated by replacing d with the corrected wheel depth of cut Expressing equation (3.10a) for shear stress in terms of actual undeformed chip thickness using equations (3 6) and (3 9), we get

$$\tau = \tau_o'\ \bar{\rho}^{-0\ 2065}\ t^{-0\ 826} \qquad (3\ 11)$$

where τ_o' is another constant

The specific energy, u, (energy required to remove a unit volume of material) can be evaluated from

$$u \simeq \frac{3\ F_t\ V}{2vbd} \qquad (3\ 12)$$

When this is plotted against t_m (Fig 20), the following relationship is obtained

$$v = u_o \, t_m^{-0.822} \qquad (3.13)$$

where u_o is a constant. Replacing t_m in terms of t and by equation (3.6b) we get

$$u = u_o' \, t^{-0.208} \, t^{-0.826} \qquad (3.13a)$$

where u_o and u_o' are constants. Equations (3.11) and (3.13a) agree with the results obtained by Armarego and Brown[26] with spherical tools. This in general also agrees with the results of Backer et al[17] for the entire wheel where the individual grains are not considered but the average of all grains is taken into account.

The increase in specific energy with decreasing values of t, can be explained in terms of 'size effect' in a similar manner as discussed by Backer et al[17] for the grinding operations. The general shape of the curve (Fig 20) also agrees with those presented by Backer et al[17]. At smaller values of t, ploughing and rubbing will also be significant and cause an increase in u.

In overcut flymilling the cutting points (grits) produce grooves of boat like shape on the surface of the workpiece. As indicated earlier the transverse section of the groove be approximated by a circular arc of radius ρ. The schematic view of the contact zone is shown in Fig. 21.

The contact stress (σ_n) between the grains and the work-piece is then given by

$$\sigma_n = \frac{8 F_n}{\pi b^2} \qquad (3\ 14)$$

and $$A_c = \frac{\pi b^2}{8} \qquad (3\ 14a)$$

where A_c is the projected contact area of the grain

Plot of maximum normal force with maximum projected area of contact (A_c), (Fig. 22) shows that the two are related and the relation can be expressed as

$$F_n = F_{n_o} A_c^{0.91} \qquad (3\ 15)$$

where F_{n_o} is a constant Thus it is reasonable to assume that $F_n \propto A_c$.

In order to show the effect of various parameters on the maximum normal force F_n, the depth of cut has been modified, keeping the maximum contact area to be the same. The constant tip radius for the grain was again taken to be 101×10^{-4} inches If we proceed in a similar manner as discussed earlier, the expression for modified depth of cut (d_m) in this case can be shown to be

$$d_m = \frac{\rho\, d}{101 \times 10^{-4}} \qquad (3\ 16)$$

Choosing a suitable class interval for the modified depth of cut, the mean values of the maximum normal force have been calculated in the class intervals and plotted against the corresponding midpoint of the class intervals of the

modified depth of cut in Fig 23 In this case also we get a relationship similar to equation (3 7) i e

$$F_n = F_n' + F_n'' d_r \qquad (3\ 17)$$

where F_n' and F_n'' are constants Using equation (3 16), equation (3 17) reduces to

$$F_n = F_n' + F_n'' \frac{\rho d}{101 \quad 10^{-4}} \qquad (3\ 18)$$

Fig 24 shows the variation of force ratio F_t/F_n with modified depth of cut It illustrates that as depth of cut increases, this ratio also increases and also shows the dependence on the grain tip radius

Fig 25 shows the variation of normal stress σ_n with projected area of contact This curve shows that σ_n remains almost constant except in the region where A_c is very small The increase in σ_n with decreasing contact area at very small values of A_c can be attributed to the size effect and also to the rubbing and ploughing action which become significant in this range The residual stresses developed near the surface of the workpiece will also contribute to this In order to understand this phenomena clearly, the maximum normal stress has also been plotted against the modified undeformed chip thickness (Fig 26) This curve also illustrates the same phenomena as given by the curve of Fig 27 After the undeformed chip thickness reaches a certain value (14×10^{-4} inch), the contact stress remains more

or less constant but below 14×10^{-4} inch, the normal stress increases with decrease in t, thus implying the size effect in this case also. The residual grinding stresses has been shown to be function of the normal stresses[27] and that the maximum surface stresses are smaller for heavy cuts than for light cut. The present results clearly indicate this phenomena.

CHAPTER IV

CONCLUSION

The forces acting on an individual abrasive grain of a grinding wheel is of considerable importance since it not only affects the wear properties of the wheel but it also indicates the energy requirements and temperature rise. Overcut flymilling appears to be a useful technique for evaluating abrasive grain performance under fine grinding conditions. Piezo-electric accelerometer appears to be a useful instrument for the purpose of measuring dynamic forces during cutting with single abrasive grains. It has been shown that the accelerometer displacement is related to the input force and thus calibration is linear over the required force range. The method of calibrating the accelerometer dynamometer by dropping balls from known heights gives consistent results.

Experiments indicate that the tangential force on a grain varies linearly with the chip cross-section area. The specific energy and shear force increases with decrease in chip size in the similar manner as reported earlier for fine grinding. Normal or contact stress on the other hand remains more or less constant with chip thickness except in the range of very fine chip thickness where it increases with decreasing chip size.

REFERENCES

1. Hahn R.S., "The effect of wheel work conformity in precision grinding". Trans. A.S.M.E., Vol. 77, 1955, p 1325.
2. Peklenik J., "Contribution to theory of grinding", Mechanical Journal, 1959, Vol. 4, p 1.
3. Hahn R.S., "On the nature of the grinding process," Proc. 2nd Int. MTDR Conf. Birmingham, England, 1962.
4. Reichenbach G.S., Mayer J.E., Kalpakchioglu S. and Shaw M.C., "The role of chip thickness in grinding", Trans. A.S.M.E., Vol. 78, 1956, p. 847.
5. Shaw M.C., "The grinding of Metals", Proc. Conf. on Tech. and Eng. Manufacture, I. Mech. E., London, 1958.
6. Snoeys R., Peters J., Werkturgkunde I.V. and Decneut A., "The significance of chip thickness in grinding", Annals C.I.R.P., Vol. 23/2, 1974, p 227.
7. Shaw M.C., "Interpretation of grinding data", Unpublished Report, Carnegie-Mellon University, Pittsburgh, U.S.A., 1972.
8. Backer W.R., Marshall E.R. and Shaw M.C., "The size effect in metal cutting", Trans. A.S.M.E., 1952, Vol. 74, p 61.
9. Khruschov M.M. and Babichev M.A., "Investigation of the wear of metals and alloys by rubbing on an abrasive surface", Friction and Wear in Machinery, Vol. 12, 1958, p 1.

10. Hahn R.S., "Controlled force grinding - A new technique for precision internal grinding," Trans. A.S.M.E., Vol. 86 B, 1964, p 287.

11. Hahn R.S., "On the mechanics of the grinding process under plunge cut conditions," Trans. A.S.M.E., Vol. 88B, 1966, p 72.

12. Hahn R.S., "Some characteristics of controlled force grinding", Advances in Machine Tool Design and Research, Vol. 6, 1965, p 591.

13. Hahn R.S., Fleischer P. and Griffith R.C., "On the selection and design of grinding cycles", Advances in Machine Tool Design and Research, Vol. 7, 1966, p 599.

14. Sato K., "Grinding temperatures", Bull. Japan Soc. Grinding Engrs. Vol. 1, 1961, p 183.

15. Jaeger J.C., "Moving sources of heat and temperatures at sliding contacts", Proc. Royal Soc. of New Southwales, Vol. 76, 1942, p 203.

16. Nakayama K. and Shaw M.C., "Study of the finish produced in surface grinding", Part-2-Analytical, Proc. Instn. Mech. Engrs., Vol. 182, 1967-68, p 179.

17. Brecker J., "Elastic effects in grinding", Ph.D. Thesis, Carnegie Institute of Technology, Pittsburgh, U.S.A., 1967.

18. Shiozaki S. and Miyashita M., "Dynamics and design of dynamometers," Annals CIRP, Vol. 18, 1970, p 363.

19. Thomson W.T., "Theory of Vibration with applications", Prentice Hall, Inc., U.S.A., 1972.

20. Kulkarni V.P., "Design and development of piezoelectric accelerometers", J. Inst. Eng. (India), Electron. Telecommun. Eng. Div., Vol. 55, 1974, p 55.

21. Timoshenko S. and Goodier J.N., "Theory of elasticity", 3rd Ed., McGraw-Hill Kogakusha Ltd., Japan, 1970.

22. Shaw M.C., Farmer D.A. and Nakayama K., "Mechanics of the abrasive cut off operation", Trans. A.S.M.E., Vol. 89, 1967, p495.

23. Marshall, E.R. and Shaw M.C., "Forces in dry surface grinding", Trans. A.S.M.E., Vol. 74, 1952, p 51.

24. Lal G.K. and Shaw M.C., "Wear of single abrasive grains in fine grinding", Proc. Int. Grinding Conf., Carnegie-Mellon University, Pittsburgh, U.S.A., 1972.

25. Alden G.I., "Operations of the grinding wheel in machine grinding," Trans. A.S.M.E., Vol. 36, 1914, p. 451.

26. Armarego, E.J.A. and Brown R.H., "On the size effect of metal cutting", Int. Jnl. Prod. Res., Vol. 3, 1962, p 75.

27. Frisch J. and Thomsen E.J., "Residual grinding stresses in mild steel", Trans. A.S.M.E., Vol. 73, 1950, p 337.

28. Lal, G.K. and Shaw, M.C., "The Role of Grain Tip Radius in Fine Grinding", Trans.ASME,Vol.97B,1975,p1119.

APPENDIX 'A'

Undeformed Chip Thickness

Over cut flymilling is shown diagramatically in Fig 3 Here the aluminum disc with abrasive grain attached to the periphery rotates with a constant rpm N and the workpiece is fed with a velocity v The geometry of the chip produced by assuming the centre of rotation of the wheel to move from A to B / The distance A B is shown in Fig 3 equal to v/N, the feed during one revolution of the workpiece

From the triangle ACE,

$$CE = \sqrt{(\frac{D}{2})^2 - (\frac{D}{2} - g)^2},$$

therefore, $DC = CE - DE$

or $$DC = \sqrt{(\frac{D}{2})^2 - (\frac{D}{2} - g)^2} - \frac{V}{N}$$

From the triangle BDC

$$BC = (BD^2 + DC^2)^{1/2}$$

where $BD = \frac{D}{2} - g$

The undeformed chip thickness at any depth g, from the start of the cut is,

$$t_g = \frac{D}{2} - BC$$

$$= \frac{D}{2} - \left[\left(\frac{D}{2} - g\right)^2 + \left(\left(\frac{D}{2}\right)^2 - \left(\frac{D}{2} - g\right)^2 - \frac{v}{N}\right)^2\right]^{1/2}$$

or $$t_g = \frac{D}{2}\left[1 - \left[1 - \frac{8v}{ND^2}\left(Dg - g^2\right)^{1/2} + \left(\frac{2v}{ND}\right)^2\right]^{1/2}\right]$$

Expanding and neglecting the higher order terms,

$$t_g = \frac{2v}{N}\left[\frac{g}{D} - \left(\frac{g}{D}\right)^2\right]^{1/2} - \frac{1}{D}\left(\frac{v}{N}\right)^2$$

Substituting g = d, maximum undeformed chip thickness may be computed. Thus,

$$t = \frac{2v}{N}\left[\frac{d}{D} - \left(\frac{d}{D}\right)^2\right]^{1/2} - \frac{1}{D}\left(\frac{1}{N}\right)^2$$

The area of cut at any depth g is shown in Fig 4, may be considered as the area between two similar circular arcs displaced by a distance t_g Thus, if it is assumed that the instantaneous width of cut b_g is large compared with the instantaneous depth of cut g, the area of cut is given to a good approximation by

$$A_g \simeq b_g \; t_g$$

Substituting for t_g and using the relationship for the chordal length of a segment of a circle to give b_g in terms of the grain tip radius, ρ, the area becomes

$$A_g = 4\,\frac{v}{N}\sqrt{\frac{2\rho(d-g) - (d-g)^2\, g}{D}}$$

Differentiating with respect to g, and equating it to zero, g may be evaluated in terms of depth of cut d for maximum area of cut. Substitution in the relation for area gives the maximum area of cut as

$$A = 4 \frac{vd}{N} \sqrt{\frac{\rho}{2D} (1 - \frac{d}{2\rho})}$$

Expanding and neglecting higher order terms of $\frac{d}{2\rho}$, we have

$$A \simeq 2 \sqrt{2} \frac{vd}{N} \sqrt{\frac{\rho}{D}}$$

TABLE 1

HINDUSTAN MILLING MACHINE SPECIFICATION

TYPE	M3U
MACHINE NO	1772
MAKE	HINDUSTAN MACHINE TOOLS LTD BANGALORE 31, INDIA
Longitudinal Traverse	900 mm
Cross Traverse	300 mm
Vertical Traverse	415 mm
Swivel of Tables to either side	45°
Number of speeds	18
Spinde speed, Range I	15 - 750 RPM
II	19 - 960 RPM
Number of feeds, Longitudinal, Cross, Vertical	18 each
Feed rates, Longitudunal and cross	10-480 mm/min
Vertical	7 5 - 360 mm/min

TABLE 2

(A)

ACCELEROMETER SPECIFICATION

TYPE	4334
S NO	301251
MAKE	BRUEL & KJAER DENMARK
Reference Sensitivity at 50 Hz at 27°c and including CABLE CAPACITY	105 pF
VOLTAGE SENSITIVITY	54 6 mV /g
CHARGE SENSITIVITY	58 9 pC/g
Capacity (including cable)	1078 pF
Maximum Transverse Sensitivity at 30 Hz	$< 2\ \%$
Physical	30 grams
Weight	30 grams
Material	Stainless Steel
Environmental	260°C
Shock Linearity	3000 g typical for 200 μsec half sine wave pulse or equivalent
Max. Shock Acceleration	6000 g typical
Magnetic Sensitivity (50-400 Hz)	$<$ 1 μV/gauss
Accoustic Sensitivity	$<$ 0 2 μV/μ bar

(B)

STORAGE OSCILLOSCOPE SPECIFICATION

TYPE	564B
S NO	B153425
MAKE	TEKTRONIX, Inc U S A
CRT Type	Electrostatic deflection
Phosphor	8 x 10 cm
Writing speed	
Basic	Atleast 100 cm/ms
Enhanced	Atleast 500 cm/ms
Storage Time	One hour or less
Erase Time	250 ms or less
CRT Cathode (AC coupled)	
Low-3 dB Frequency	1 8 kHz or less
Maximum Input voltage	150 V
Remote (storage) control	
Input	
Half Screen Erase	
Pulse Initiated Erase	Negative pulse of 5V to 100V Rate of change at least 0 1V/μs
Temperature Operating	0°C to + 50°C
Line Frequency Range	48 to 440 Hz

(C)

MICROPHONE AMPLIFIER SPECIFICATION

TYPE	2603
MAKE	BRUEL & KJAER DEN MARK

Frequency characteristics

"Linear" 2 Hz to 40000 Hz to within ± 0.5 dB relative to 1000 Hz

Sensitivity	Maximum 100 μV and minimum 1000V for full deflection on the indicating meter
Meter Range	Variable in steps of 20 dB. Accuracy within ± 0.15 dB relative to position "10 mV" and 1000 Hz
Range Multiplier	Variable in steps of 10 dB Accuracy within ± 0.1 dB relative to position "X0.01" and 1000 Hz
Distortion	Within 0.1% in the frequency range 5-40000 Hz, loaded with a load higher than 500 Ω

(D)

VIBRATION PICK-UP PREAMPLIFIER SPECIFICATION

TYPE	1606
MAKE	BRUEL & KJAER DEN MARK
Frequency Range	0.2 Hz to 100000 Hz within ± 0 5 dB when "Sensitivity Adjustment" is set to "0"
Amplification	Maximum 38 dB approx Voltage amplification when set for acceleration measurement
Max. Output voltage	In condition "Acceleration" 20 V peek when "Sensitivity Adjustment" is in position "10"
Power supply	100 to 240 volts, 50 or 60 Hz

TABLE 3

MECHANICAL AND PHYSICAL PROPERTIES OF WORK-PIECE AND CALIBRATION BALL

	Workpiece	Ball
Material	Mild Steel	Stainless Steel
Radius of curvature (mm)	∞	1 75
Weight (gm)	∞	0 239
Poisson's Ratio (μ)	1/3	1/9
Young's Modulus (E) Psi	29×10^6	28×10^6

TABLE 4

CUTTING CONDITIONS

Grain Type	Brown Al_2O3
Grain size	14
Workpiece Material	Cold Rolled Mild Steel
Table speed mm/min	60
Wheel speed RPM	25
Wheel Diameter mm	264

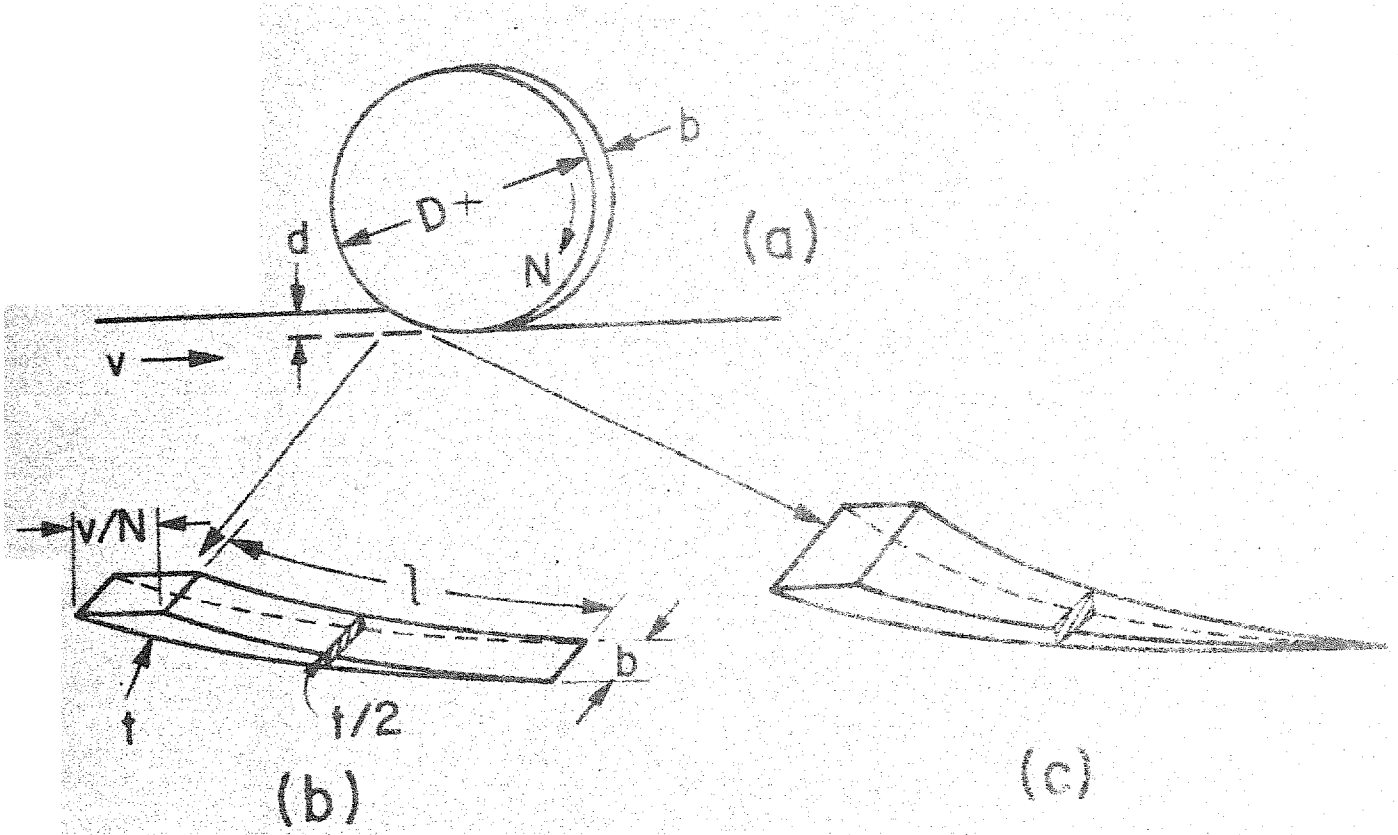

Fig. 1 Individual Chips Produced In Surface Grinding
a) Schematic view of process
b) Idealized chip used to insure volume continuity
c) Actual shape of undeformed chip

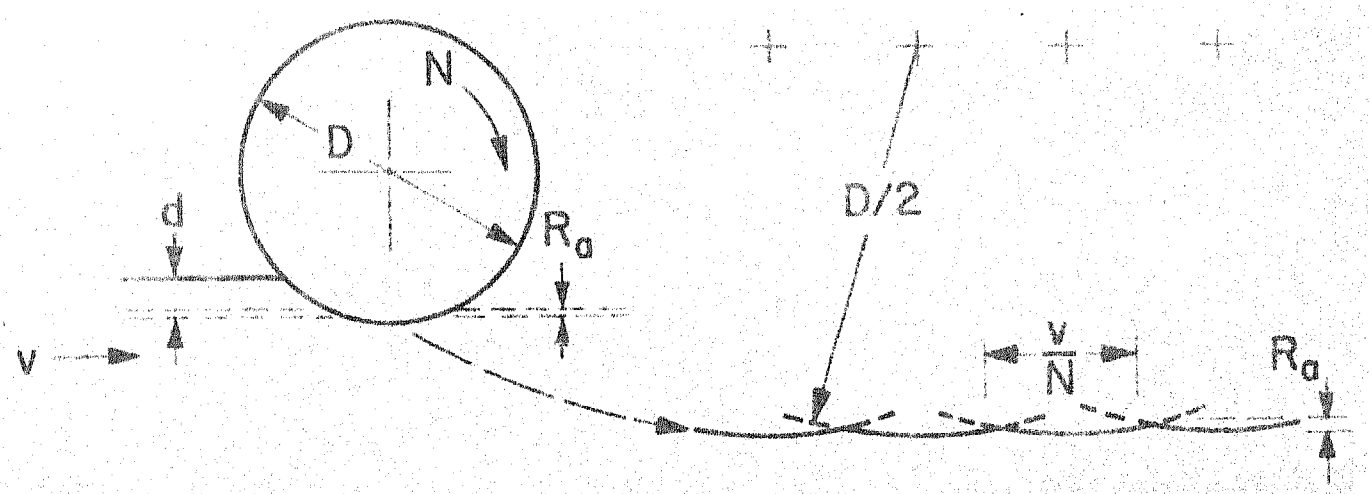

Fig.2(a) Source Of Scallops Of Height R_a On Ground Surface

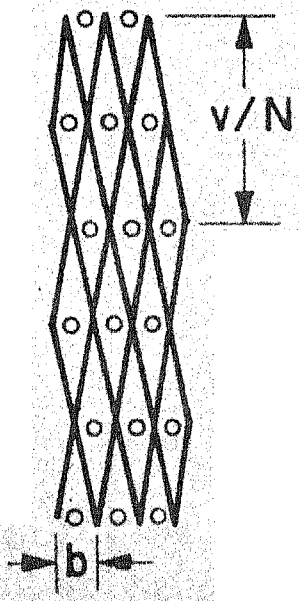

Fig.2(b) Plan View Of Scratches Left On Ground Surface By Wheel Having Uniformly Spaced Active Grains

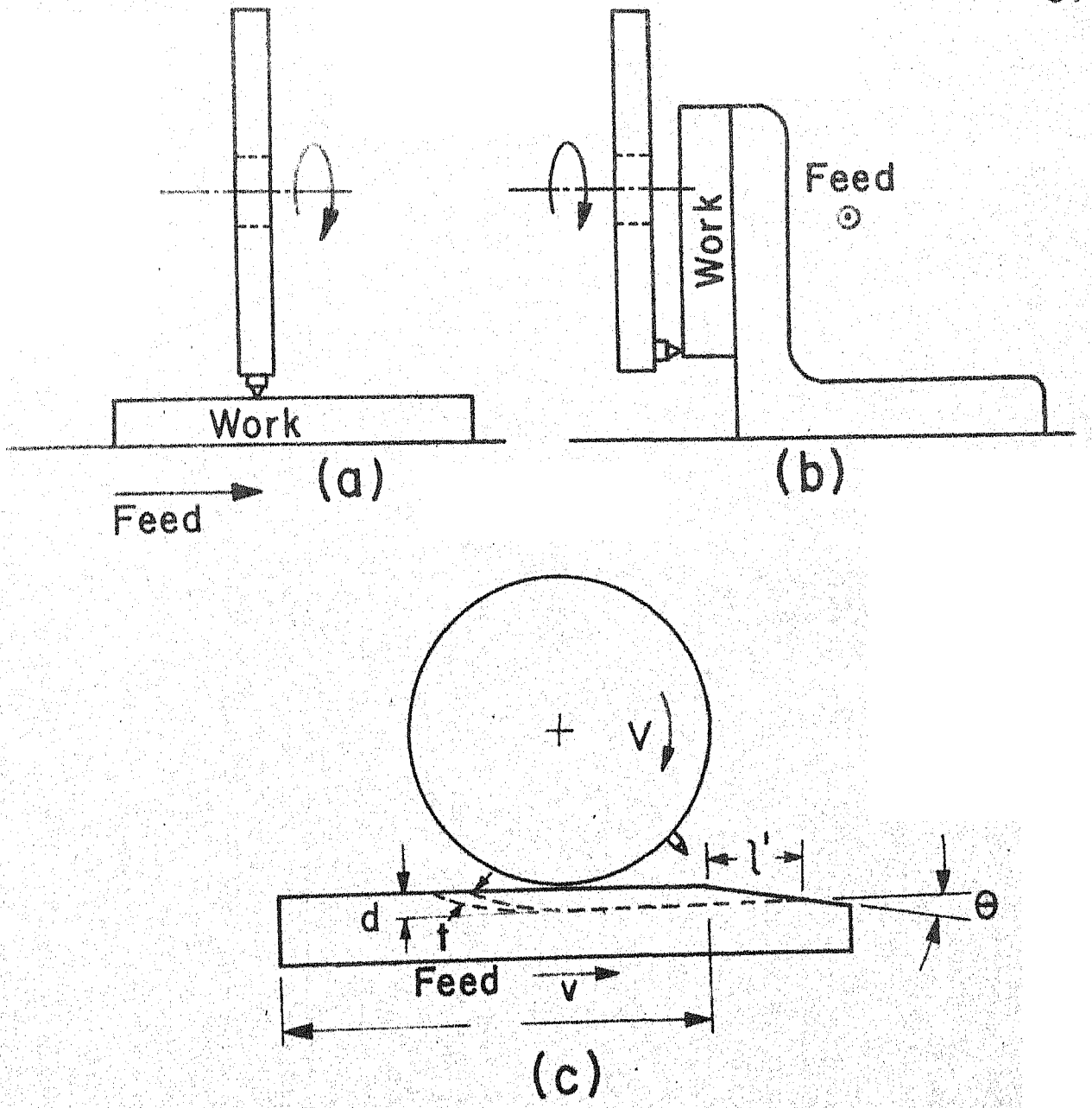

Fig. 3 Diagramatic Sketches Showing (a) Plane Flymilling, (b) Face Milling And (c) Overcut Fly-milling.

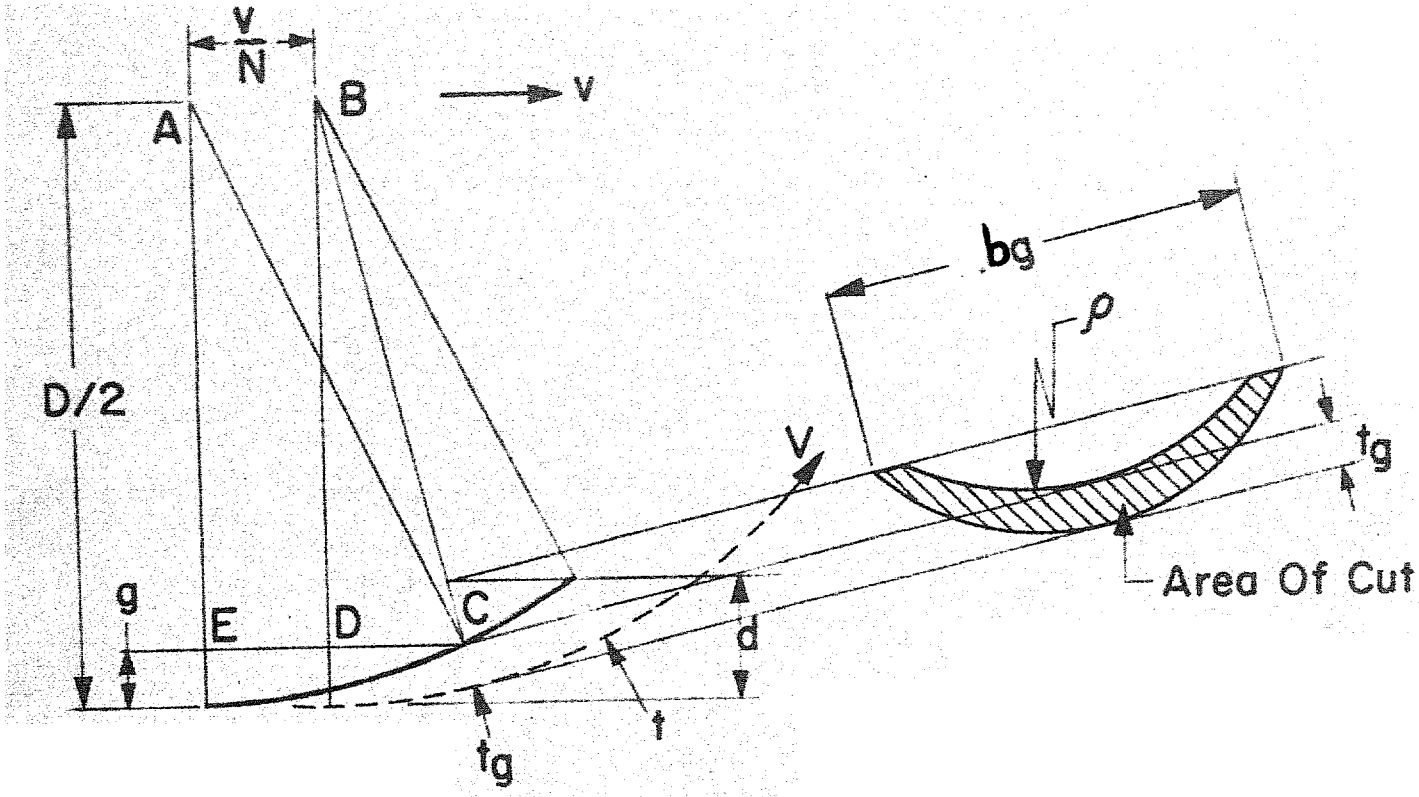

Fig.4 Geometry Of Chip Formation And Chip Area Of Cut For Spherical Tools

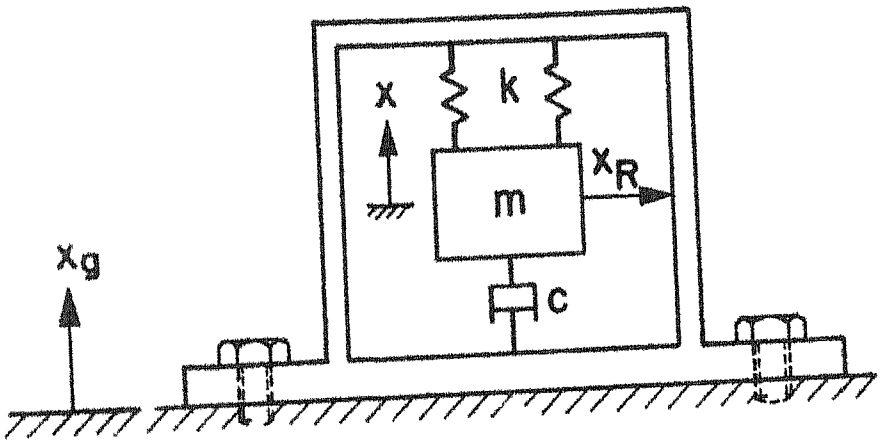

Fig.5 Diagramatic Sketch Showing Idealised Model Of Dynamometer

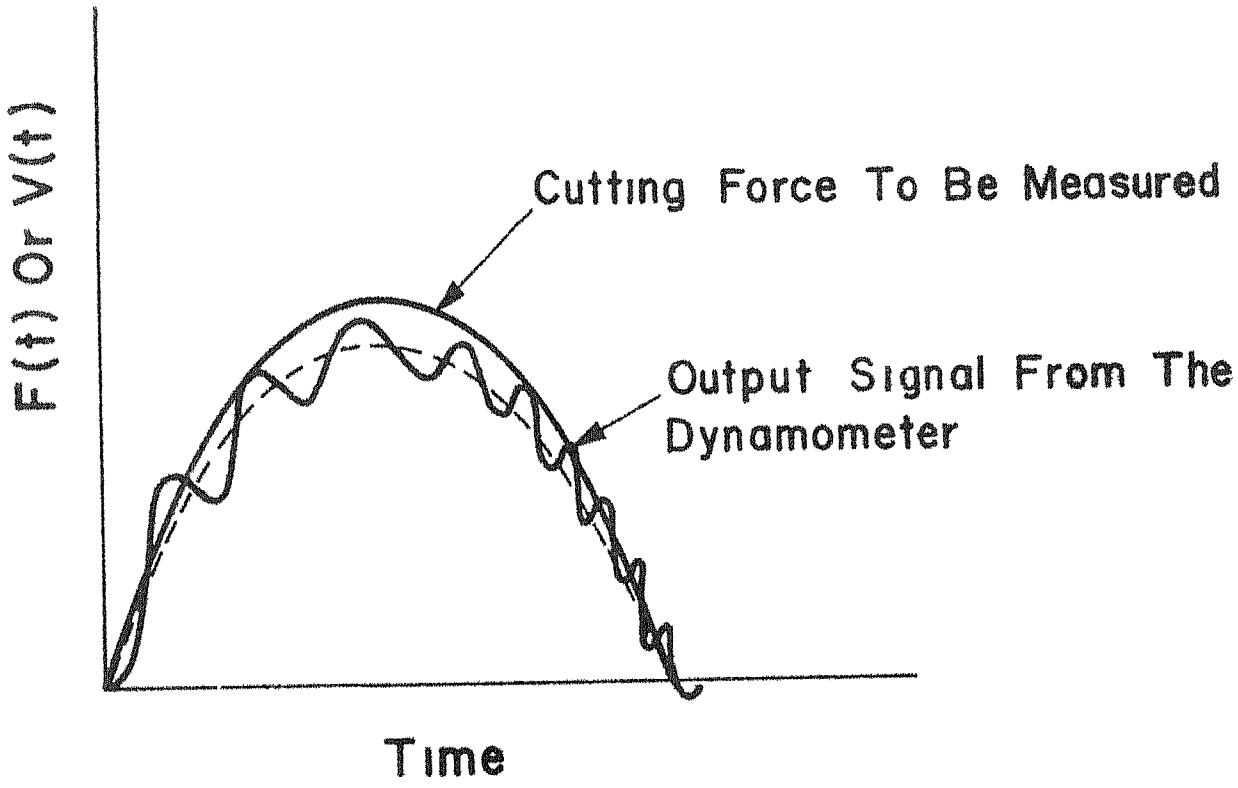

Fig 6 Cutting Force F(t) Assumed And Possible Output Signal V(t) From The Accelerometer - combined Dynamometer

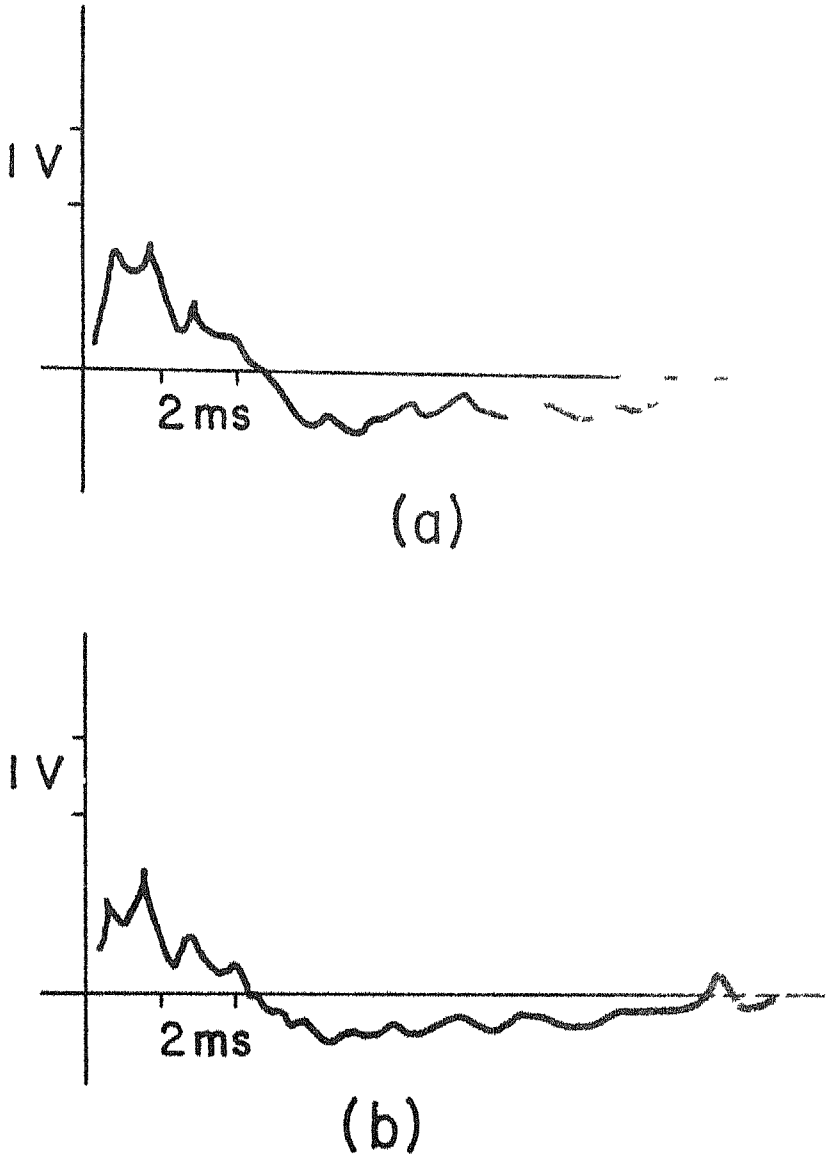

Fig 7 Typical C R O Trace
(a) Normal
(b)Tangential Components Of
The Grinding Force

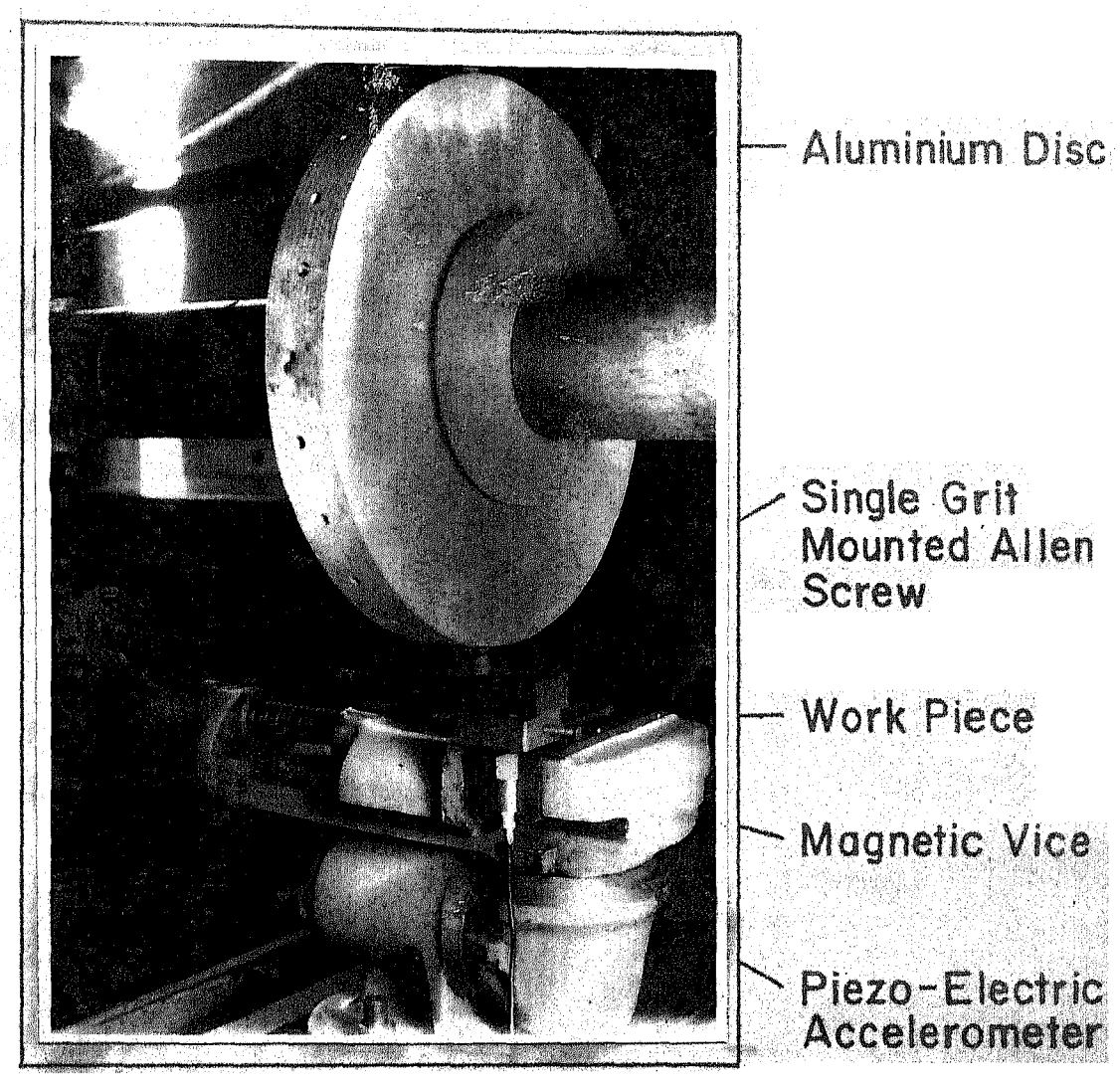
Aluminium Disc
Single Grit Mounted Allen Screw
Work Piece
Magnetic Vice
Piezo-Electric Accelerometer

Fig. 8 (a)

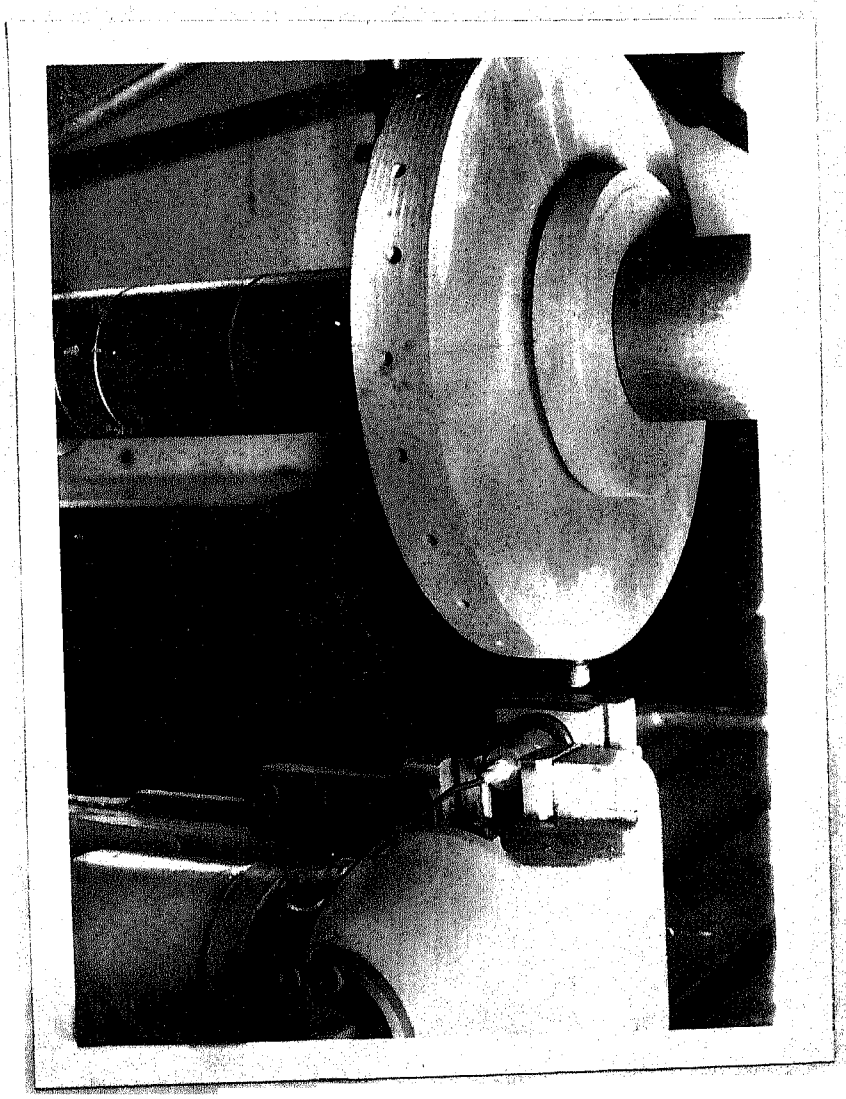

Fig. 8 (b)

Fig. 8 A Close-up View Of The Dynamometer For Measurement Of (a) Normal, (b) Tangential Component Of Cutting Forces

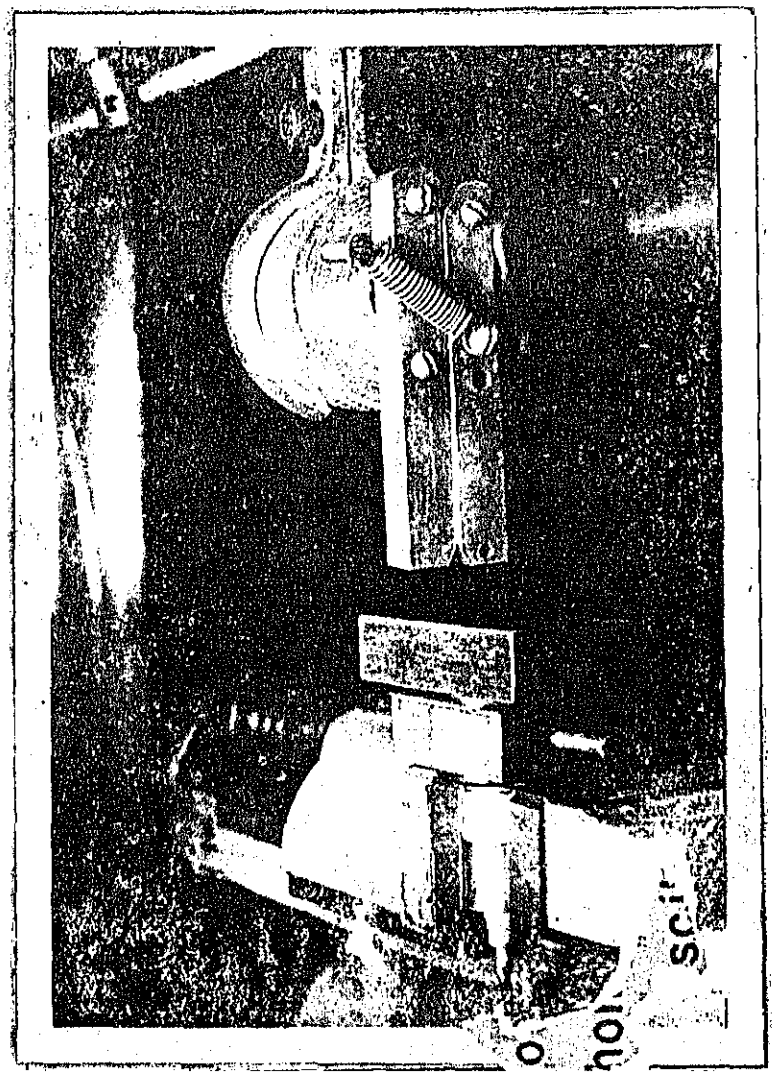

Ball Drop Device

Single Grit Mounted Allen Screw

Work Piece

Magnetic Vice

Piezo-Electric Accelerometer

Fig.10 A Close-up View Of Ball Drop Device For Calibration Of Dynamomete

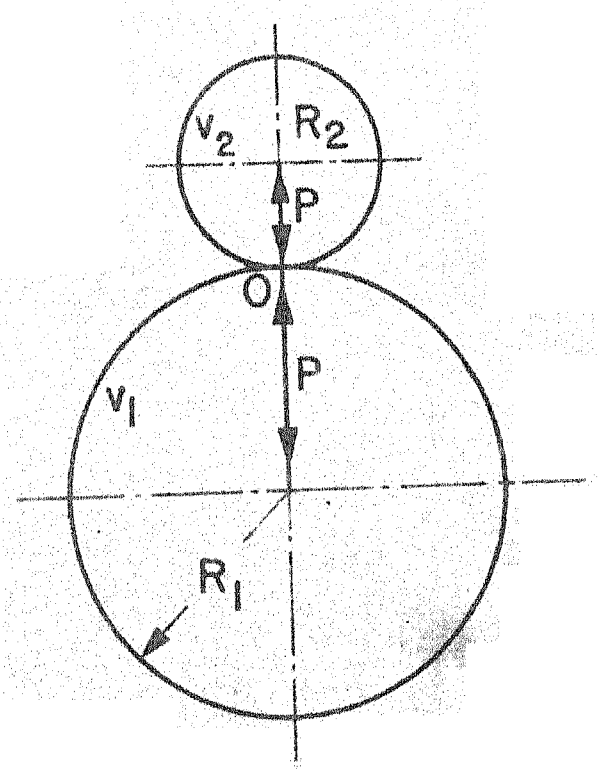

Fig. 11 Impact Of Two Spheres

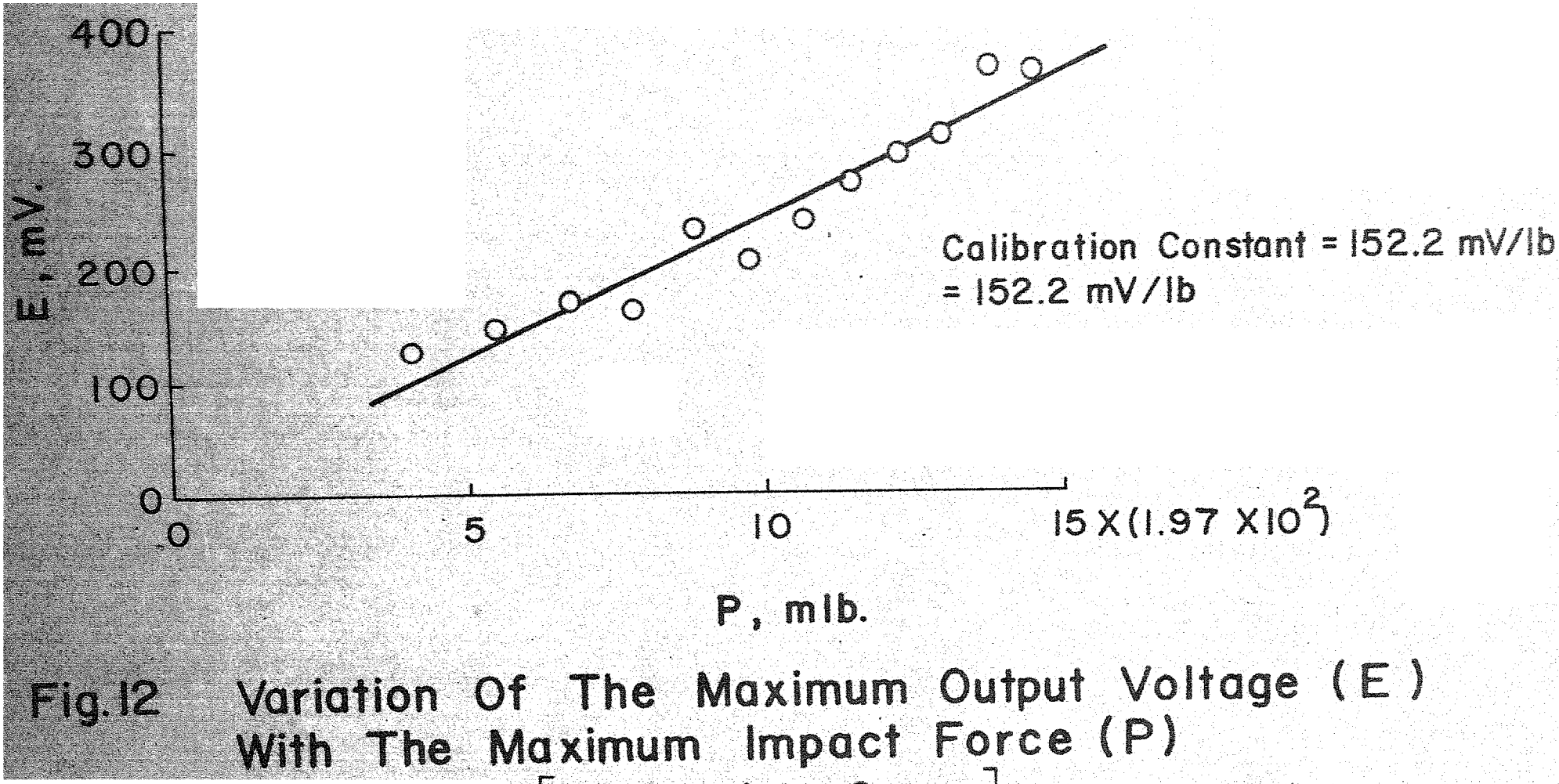

Fig.12 Variation Of The Maximum Output Voltage (E) With The Maximum Impact Force (P) [Calibration Curve]

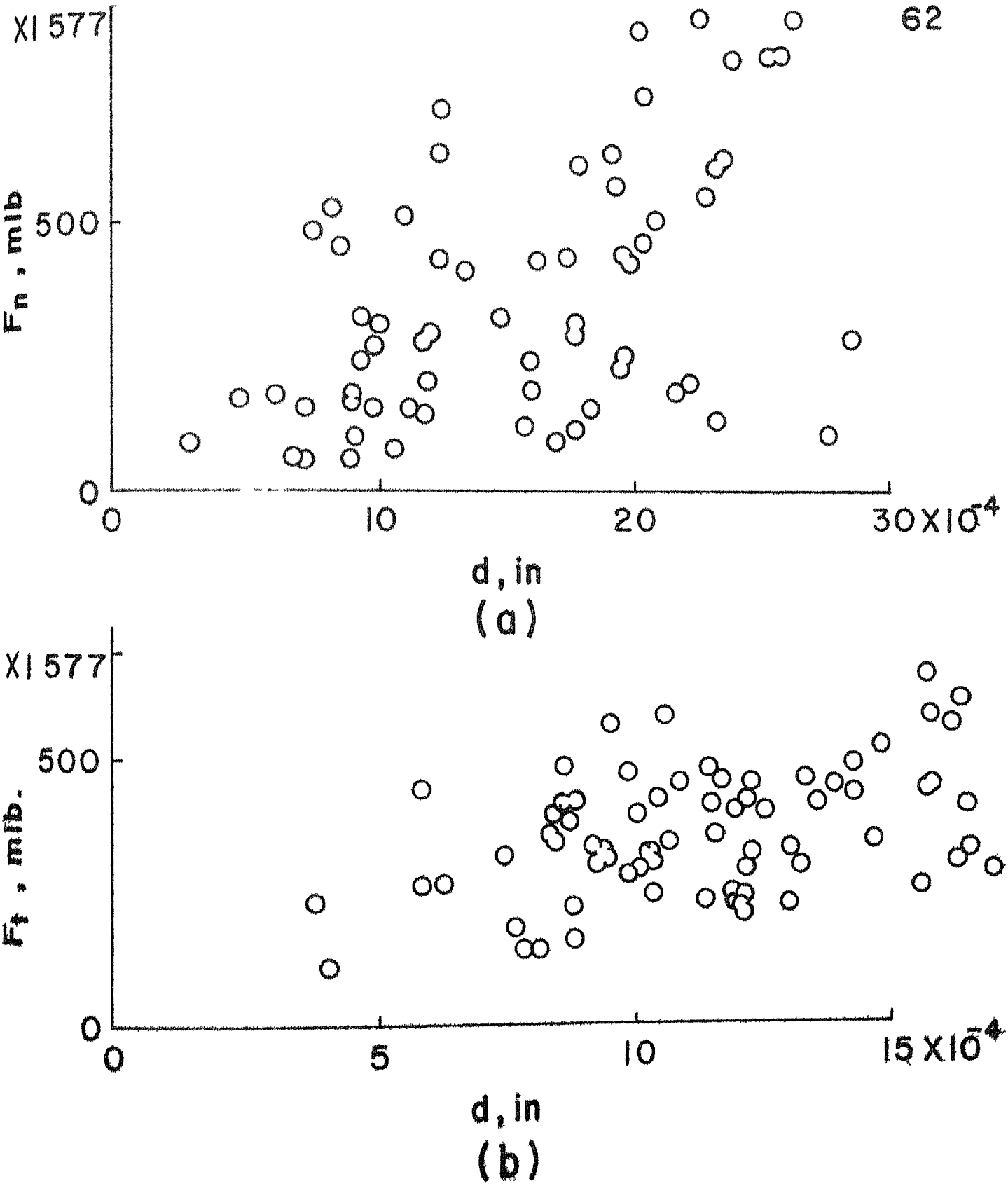

Fig.13 Scatter Diagram Of (a) Normal Force(F_n) (b) Tangential Force (F_t) With Depth Of Cut (d)

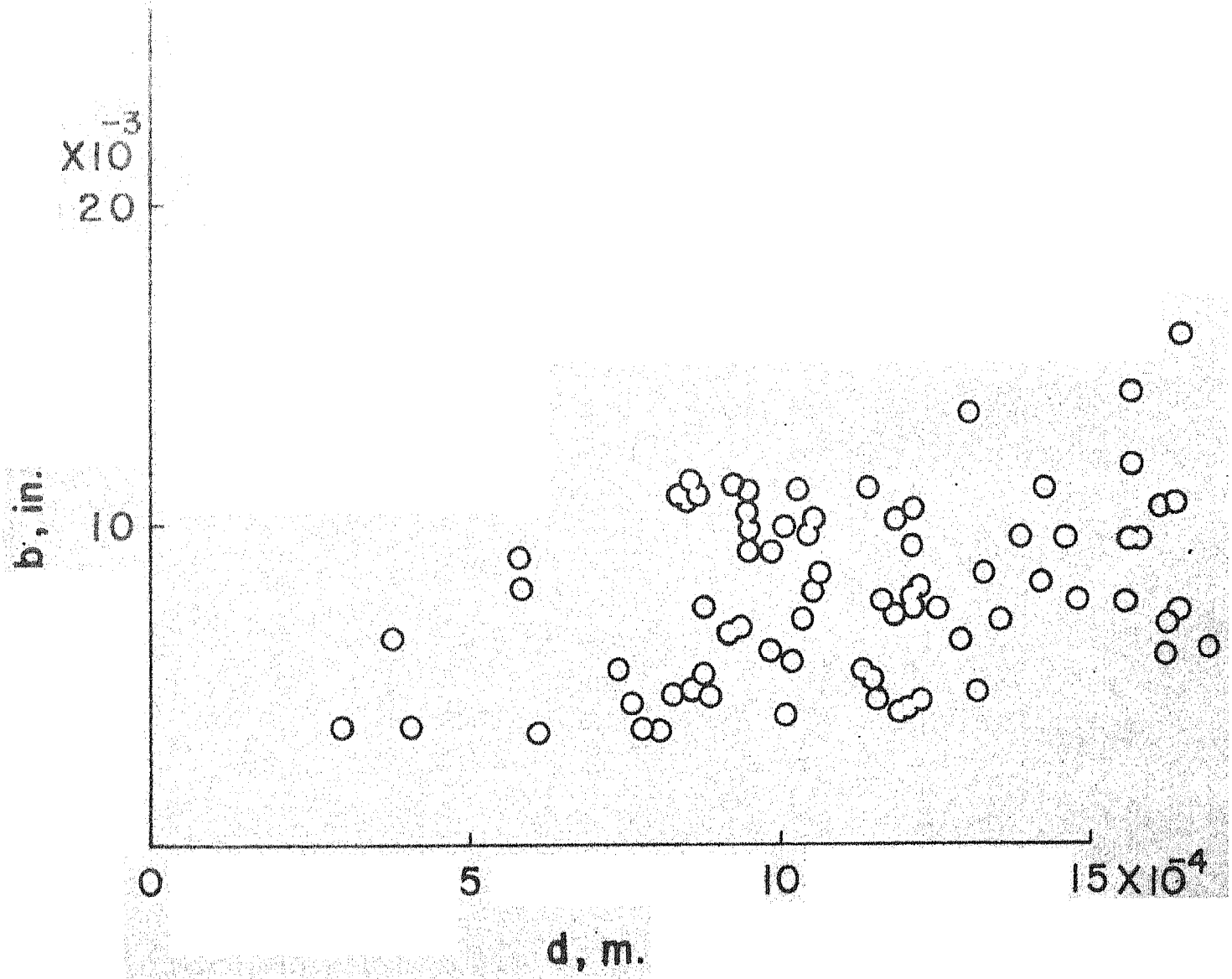

Fig.14 Scatter Diagram Of Width Of Cut (b) With Depth Of Cut (d).

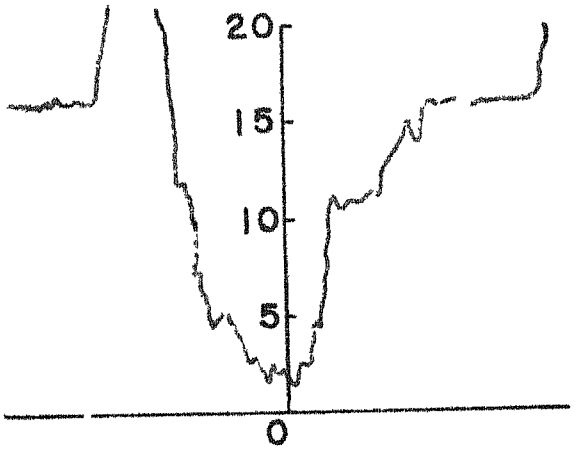

(a)

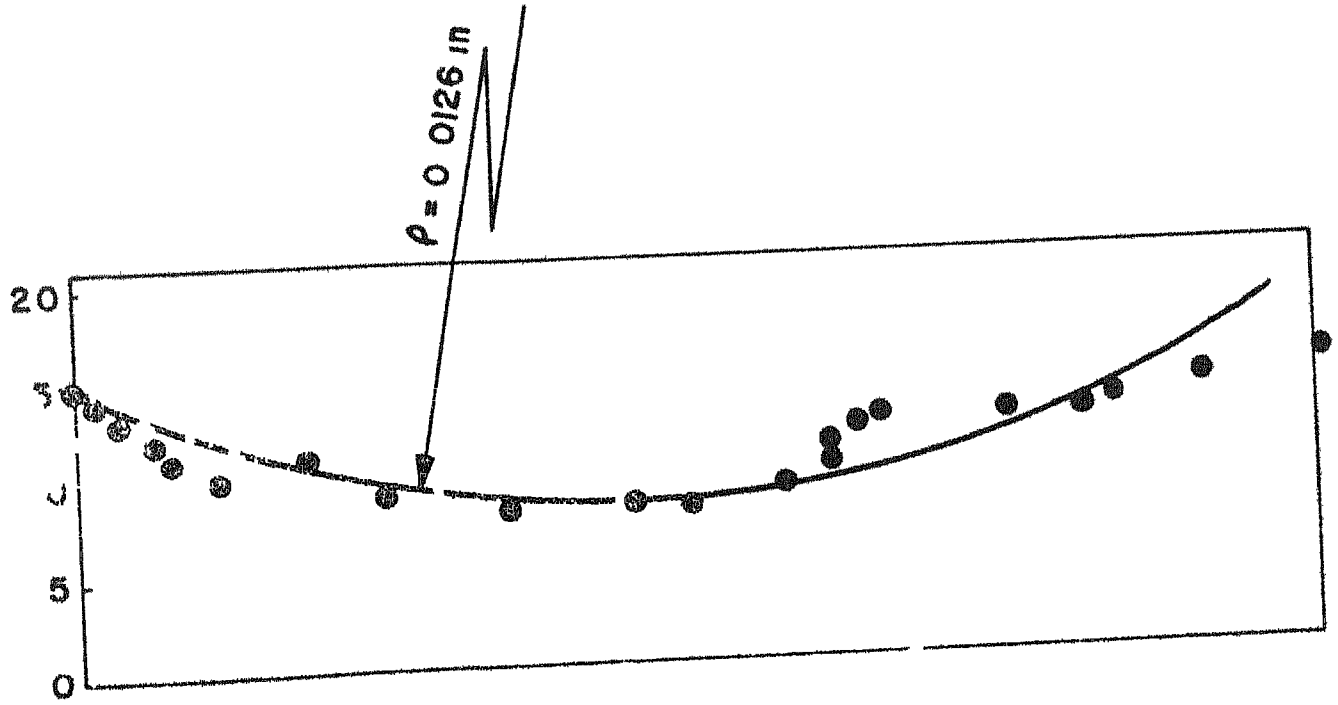

(b)

Fig. 15 (a) Grain. C-34, Wheel Speed 22,000 fpm, Table Speed. 120 ipm; Material AISI 1020, Scale Hor 1 Div = 2000 μin; Vert 1 div = 100 μin

(b) Transverse Shape Of Overcut Fly Milling Grooves With Circular Arc Passing Through Points From Talysurf Trace AISI 1020 Steel [After Lal And Shaw(28)]

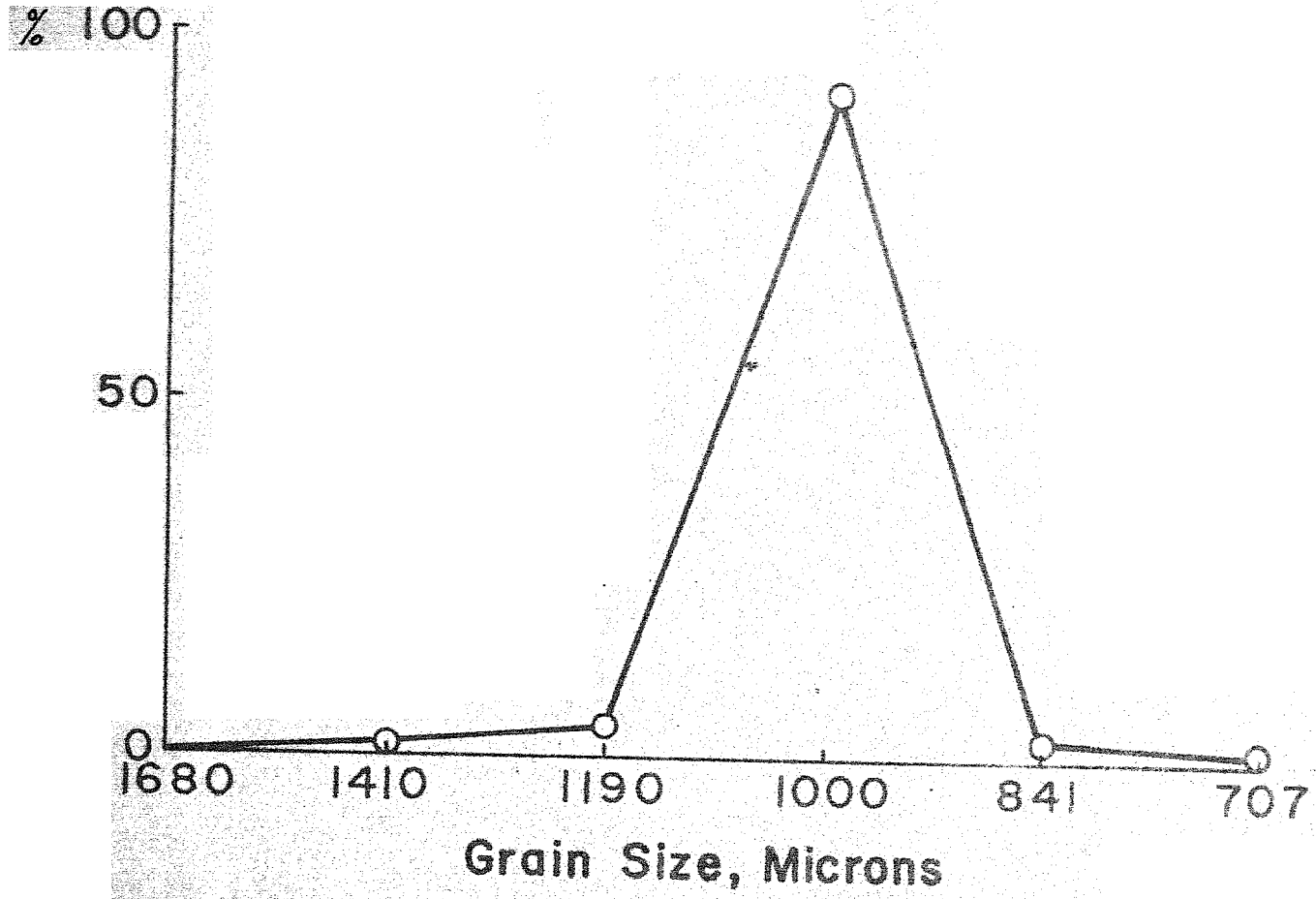

Fig. 16 Particle Size Distribution Of Brown Al_2O_3 Grit 14.

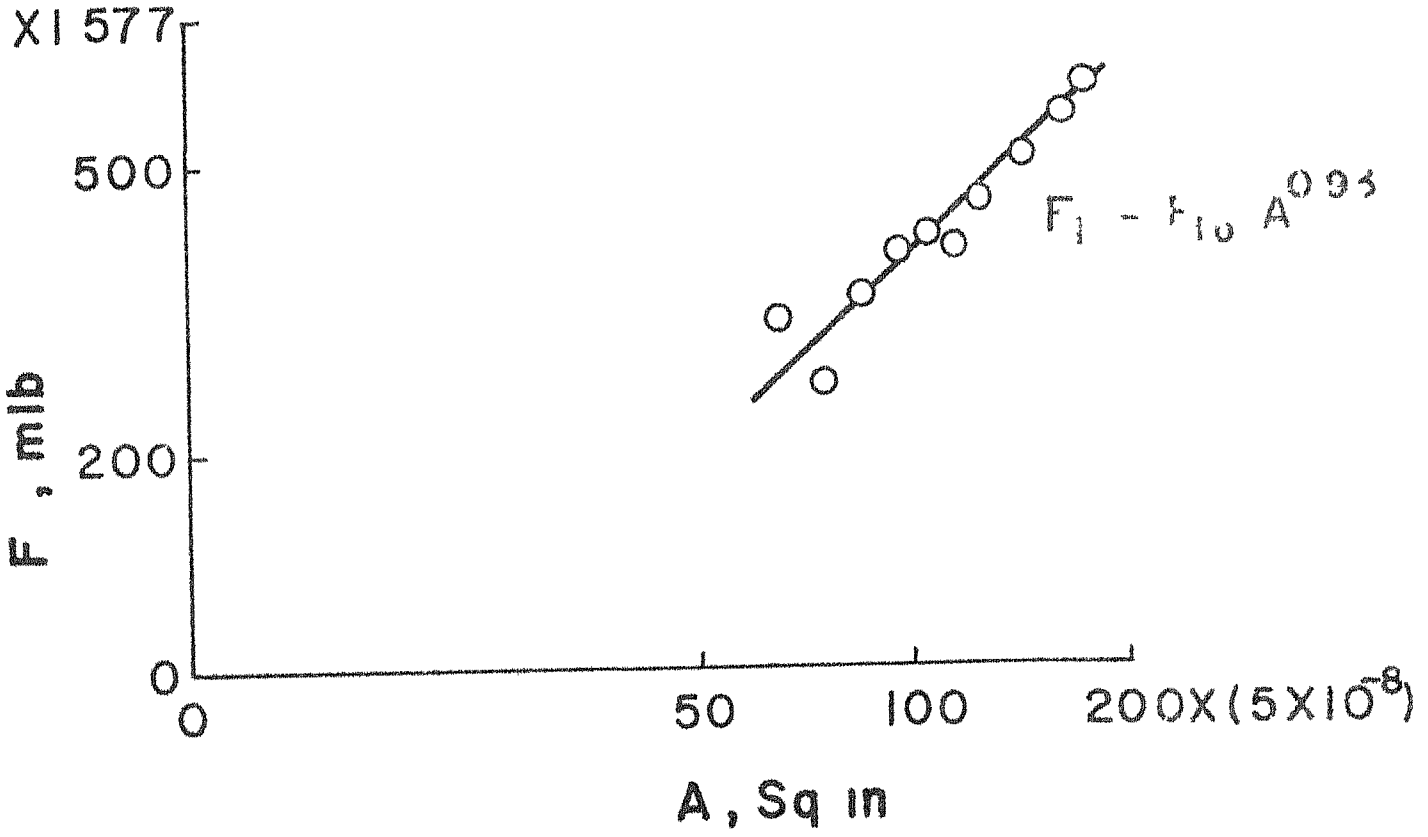

Fig 17 Variation Of Tangential Force (F_t) With Chip Cross-sectional Area (A)

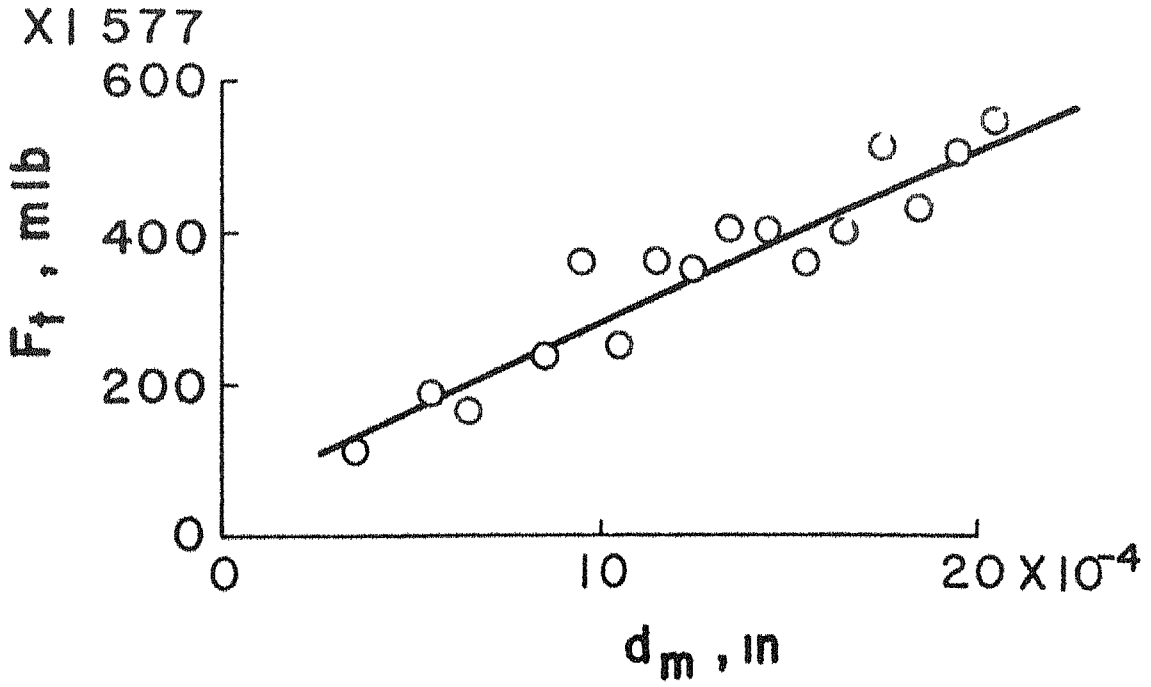

Fig.18 Variation Of Tangential Force (F_t) With Modified Depth Of Cut (d_m)

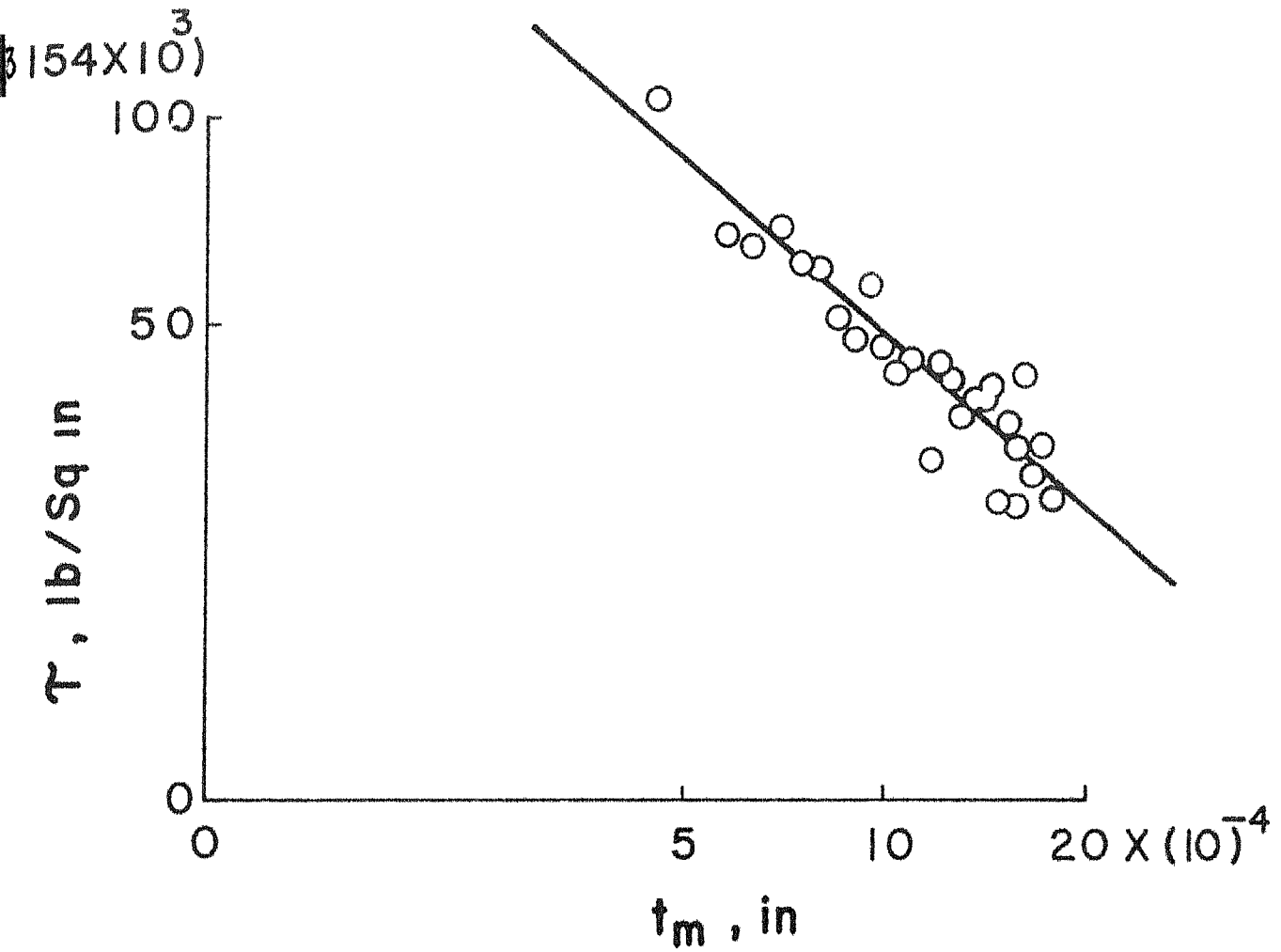

Fig. 19 Variation Of Shear Stress (τ) With Modified Undeformed Chip Thickness (t_m).

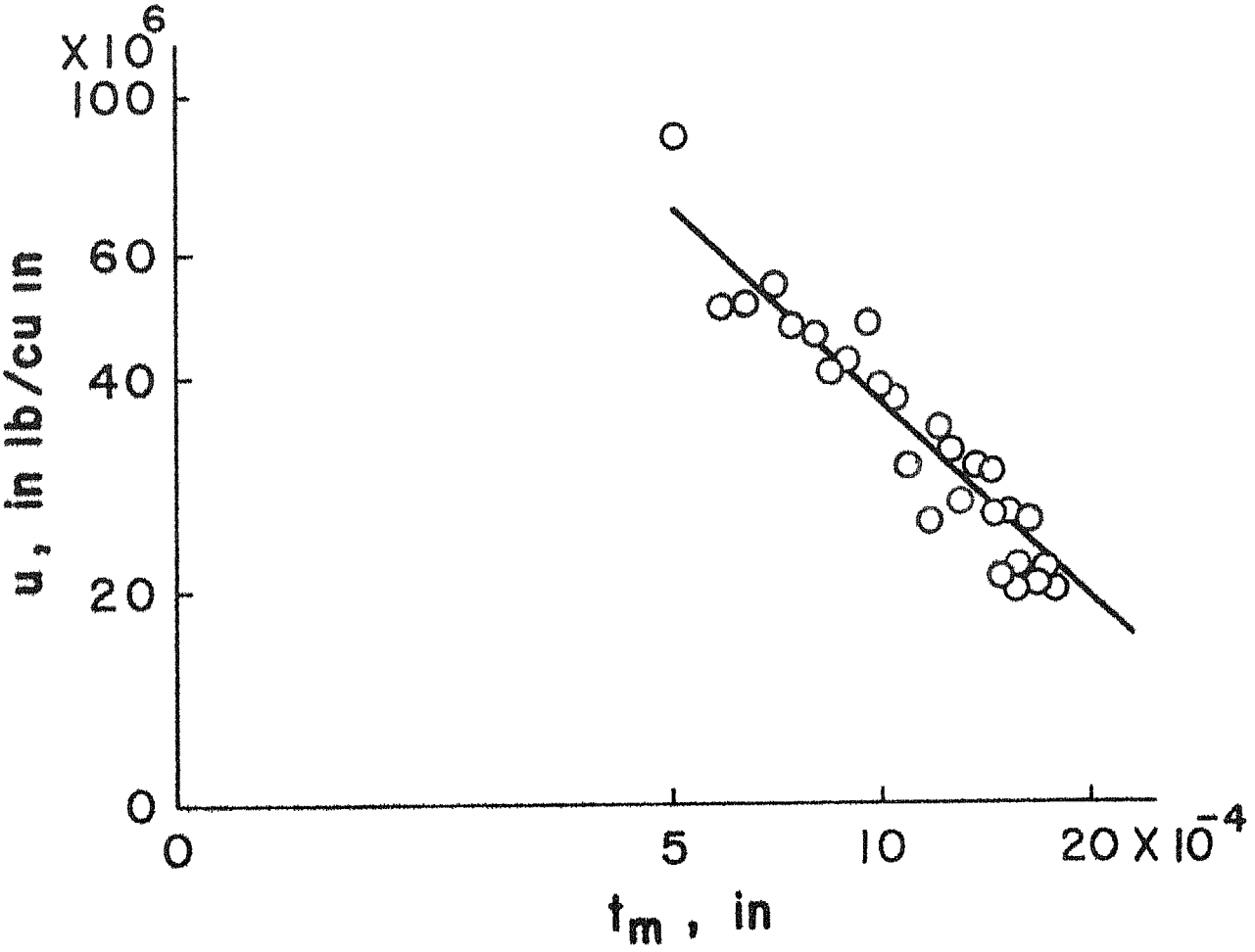

Fig 20 Variation Of Specific Energy (u) With Modified Undeformed Chip Thickness (t_m).

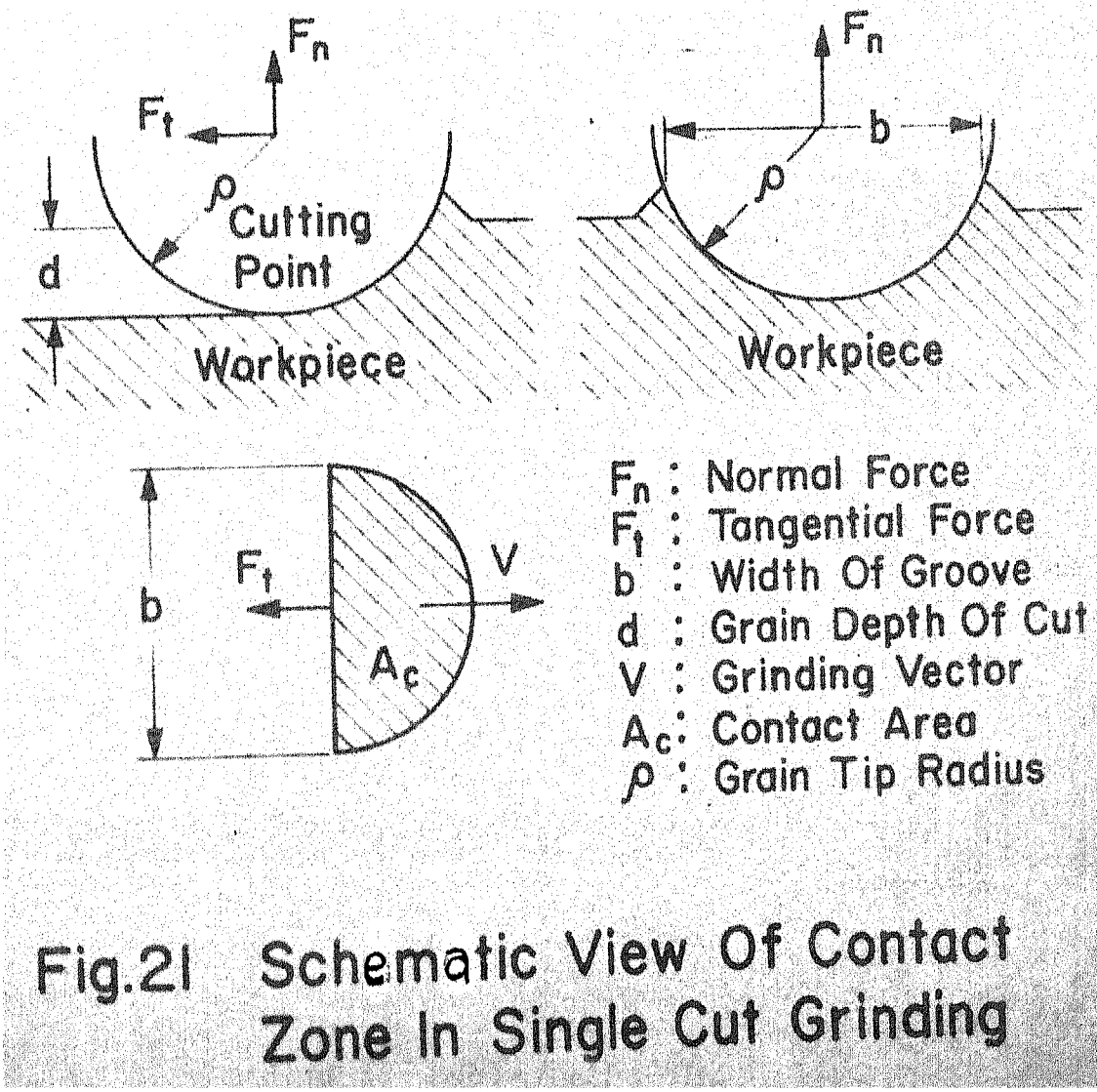

Fig.21 Schematic View Of Contact Zone In Single Cut Grinding

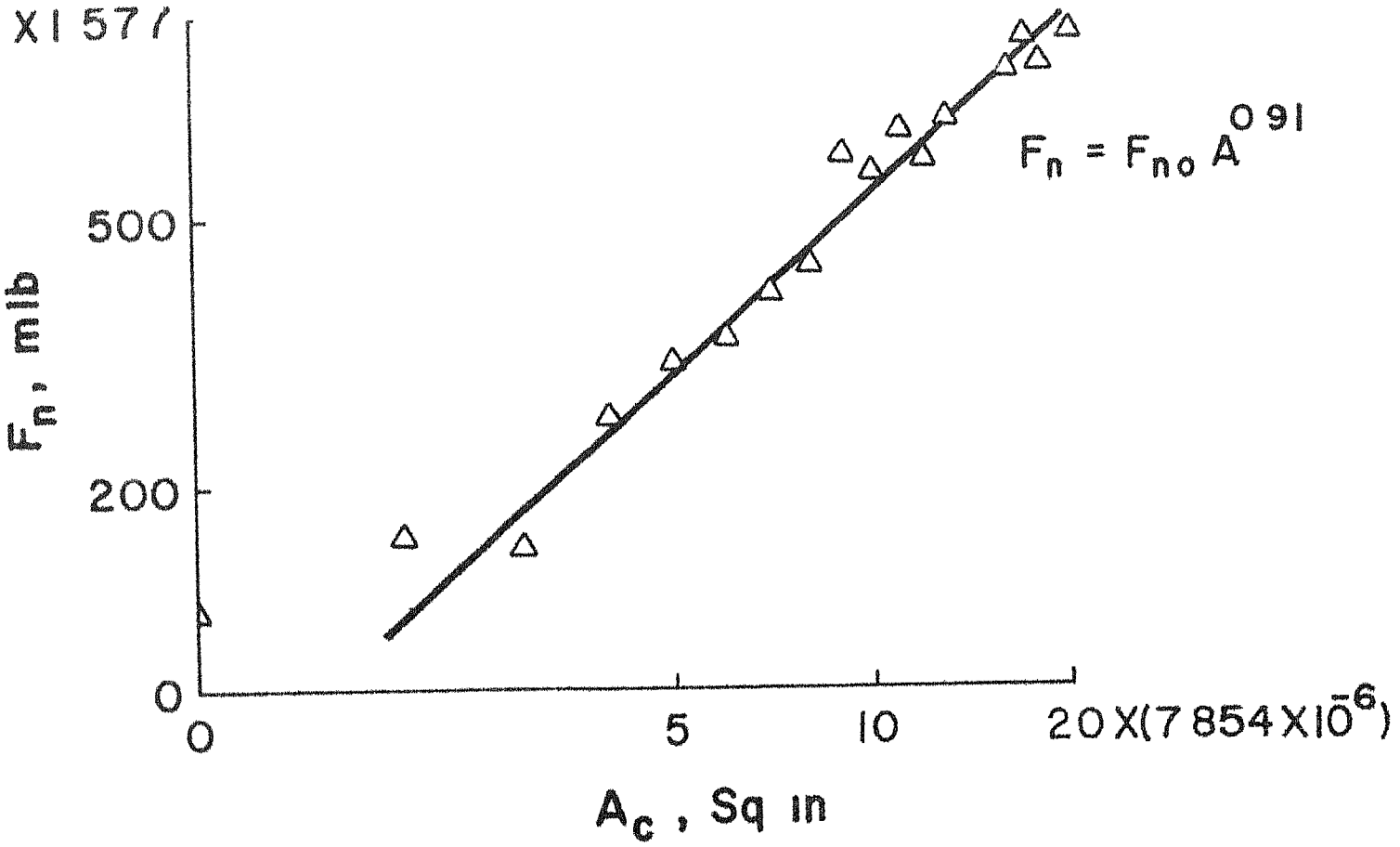

Fig 22 Variation Of Normal Force (F_n) With Projected Area (A_c)

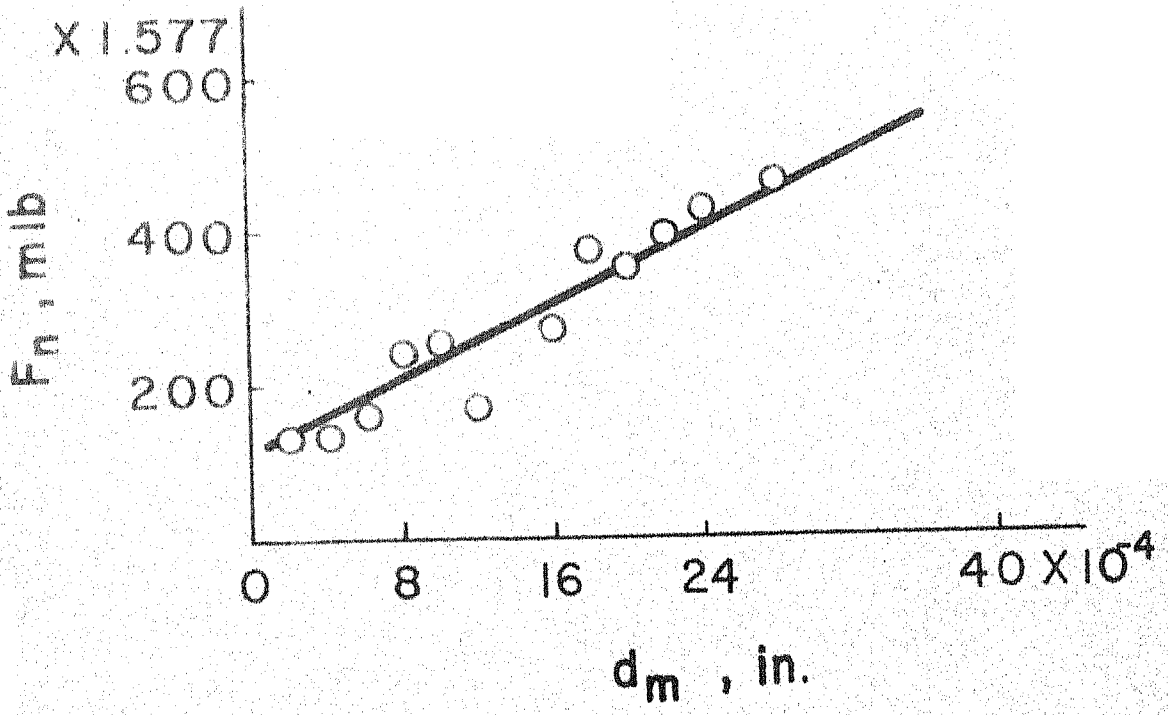

Fig. 23 Variation Of Normal Force (F_n) With Modified Depth Of Cut (d_m)

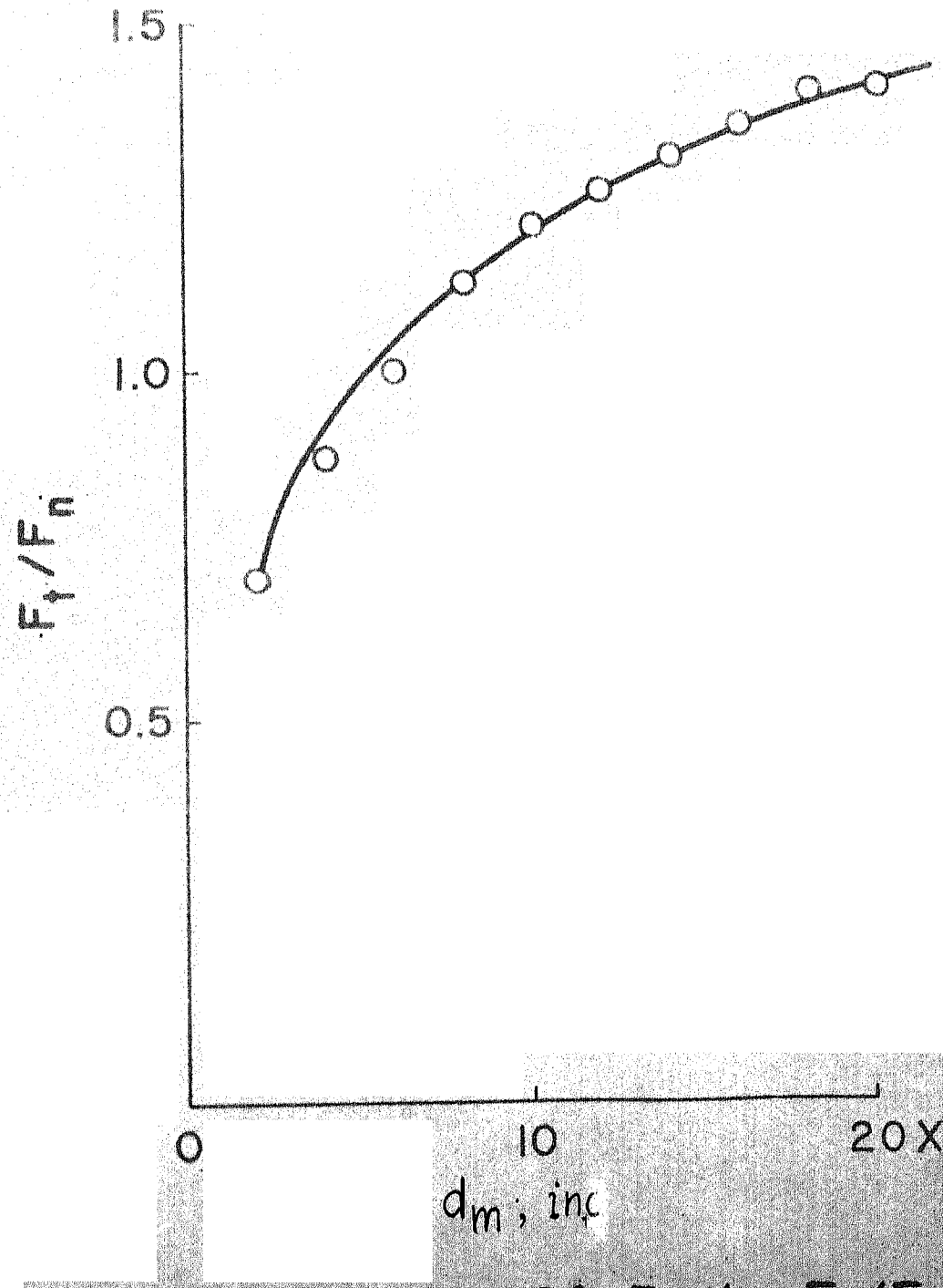

Fig.24 Variation Of Ratio F_t/F_n With Modified Wheel Depth Of Cut (d_m)

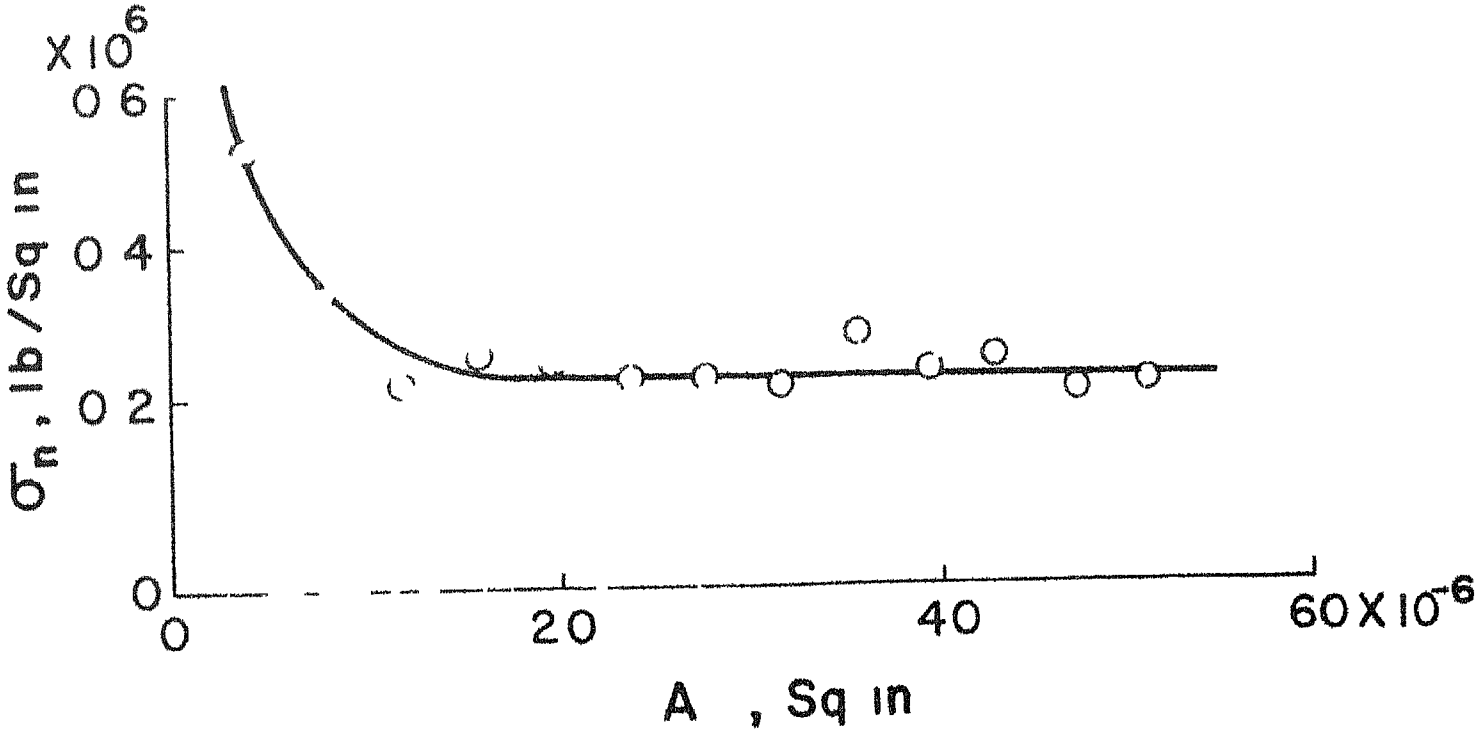

Fig 25 Variation Of Normal Stress (σ_n) With Projected Area (A_c)

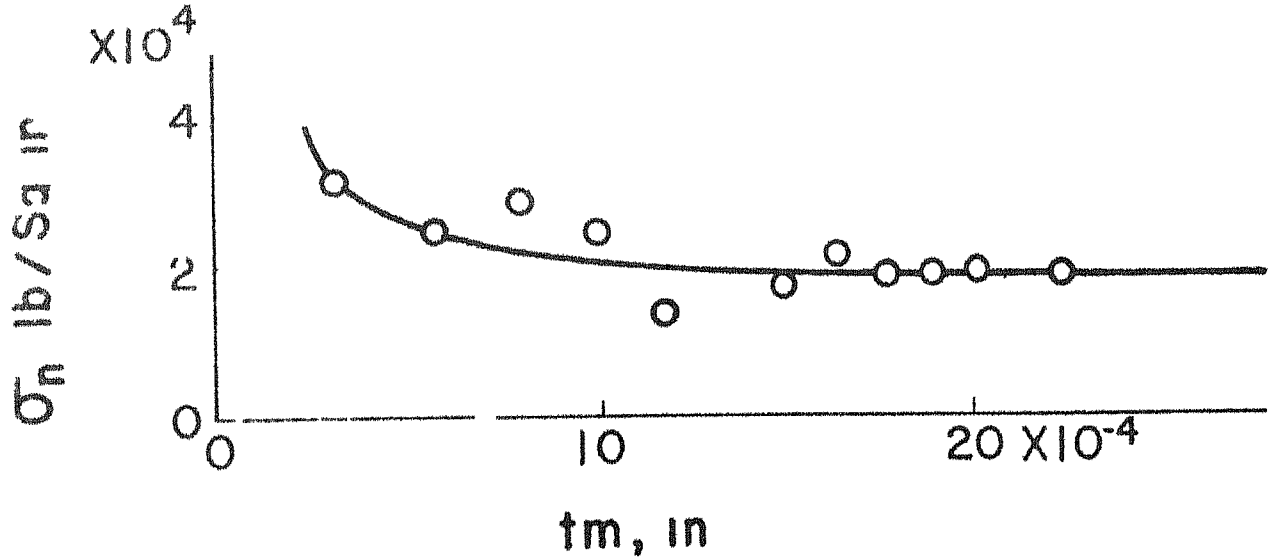

Fig 26 Variation Of Normal Stress (σ_n) With Modified Depth Of Cut (t_m)